UNIVERSITA' DEGLI STUDI "G. d'Annunzio"

Chieti-Pescara

SCUOLA SUPERIORE "G. d'Annunzio"

DOTTORATO DI RICERCA IN

Medicina Traslazionale

CICLO

XXXVIII

IMPAIRED MITOCHONDRIAL QUALITY CONTROL (MQC) DRIVES THE RELEASE OF MITOCHONDRIA-DERIVED VESICLES IN PANCREATIC DUCTAL ADENOCARCINOMA (PDAC)

Dipartimento di Medicina e Scienze dell'Invecchiamento

Settore Scientifico Disciplinare BIOS13/A

Dottorando

Dott.ssa Valentina Giansante

Coordinatore

Prof.ssa Francesca Santilli

Tutor

Prof.ssa Roberta Di Pietro

Anni Accademici 2022/2025

Index

1. Introduction 4

1.1 Pancreatic Cancer: a "silent killer" 4

1.2 The vital interplay between PDAC and Tumor Microenvironment 4

2. Mitochondrial homeostasis: a hard affair 6

2.1 Mitochondrial Quality Control System (MQC): the Guardian of Mitochondrial Safety 6

2.2 Mitochondria-derived vesicle (MDVs): additional layers of mitochondrial quality check 7

2.3 An alternative route for MDVs: the delivery into the extracellular space 8

3. Mitochondrial Dysfunction in Cancer: how does it manifest? 9

3.1 Defects of mitochondrial TCA cycle and oxidative phosphorylation 10

3.2 Generation of ROS 10

3.3 Disruption of morphological integrity 11

3.4. mtDNA alterations 11

3.5 Dysregulation of MQC 12

4. **The Ability Of Pancreatic Cancer (PC) To Drive The Activity Of Mitochondria** 13

4.1 The role of Tumor Microenvironment (TME) in PC 13

4.2 The contribution of mutated RAS proteins in respiratory injury of PC 14

5. Horizontal Mitochondrial Transfer: a new emerging strategy of intercellular communication 15

5.1 The tendency of stressed cells to "commission" the removal of dysfunctional mitochondria. 16

5.2 The contribution of neighboring cells in providing healthy mitochondria 17

5.3 Circulating cell-free mtDNA (cf-mtDNA) 17

6. Recent Findings and Aim of the Study 18

6.1 New Insights into the Clear Cell Carcinoma of the Pancreas (CCCP) 18

6.2 Aim of the Study 19

7. Materials and Methods 20

7.1 Human Cell Cultures 20

7.2 Extracellular Acidification Rate (ECAR) and Oxygen Consumption Rate (OCR) 21

7.3 3D human patient-derived Organoid (PDO) Culture 21

7.4 Gene-set-enrichment analysis (GSEA) 22

7.5 ATP and Oligomycin/2DG Dose-Response Growth Measurements 22
7.6 Immunofluorescence Assay 22
7.7 Transmission Electron Microscopy (TEM) 23
7.8 Collection of cell-conditioned media and purification of EVs 23
7.9. mtDNA Quantification 24
7.1.1 Flow Cytometry analysis of extracellular vesicles 25
8. Results 26
8.1 Human Pancreatic Cancer Cell Lines differently reprogram their energetic metabolism. 26
8.2 Comparative Analysis of EV Secretomes Highlights Increased Mitochondrial EVs in PDAC Cells 29
8.3 Patient-Derived Organoids (PDOs) can mitigate the elimination of mitochondria 32
8.4 Patient-derived organoids carrying mitophagy defects preferentially activate the Warburg effect. 35
8.5 *Inhibition of* $KRAS^{G12D}$ *Promotes Autophagy Activation and Modulates Extracellular Vesicle Trafficking in Glycolytic PDOs* 37
8.6 Increased PINK-1 signal on OMM following MRTX-1133 treatment supports a role in mitophagy 39
9. Discussion 41
References 46

1. Introduction

1.1 Pancreatic Cancer: a "silent killer"

Pancreatic Cancer (PC) is the seventh leading cause of cancer-related death, but it is expected to become the second one by 2030 (1). The lack of specific symptoms combined with the aggressive biology, contribute to the poor prognosis of pancreatic cancer, leading to its designation as a "silent killer" (2). Regarding the risk factors, cigarette smoking represents that with the strongest association with pancreatic cancer (3), followed by alcohol use (4), inflammatory diseases such as chronic pancreatitis (5) and, moreover, diet and diabetes (6). Among the different types of PCs, Pancreatic Ductal Adenocarcinoma (PDAC) accounts for more 90% of all cases, showing an overall 5-year survival rate of less than 5% and a median survival time of less than 6 months if untreated (7). The molecular profiling of PDAC involves multistep genetic alterations occurring on *KRAS, CDKN2A, TP53* and *SMAD4* genes. Low-grade precancerous lesions, known as pancreatic intraepithelial neoplasms (PanINs), can initially show *KRAS* mutations and then progress to grade 2 and 3 by acquiring additional variants for *CDKN2A, TP53* and *SMAD4* genes (8). Indeed, germline mutations occurring in *BRCA1, BRCA2* (hereditary breast and ovary cancer syndrome), and *ATM* (ataxia telangiectasia syndrome) are also associated with an increased risk for PDAC (9). However, the reason of such aggressiveness is the sum of many factors: among them, the "desmoplastic reaction" has been designated as a critical tumor hallmark (10).

1.2 The vital interplay between PDAC and Tumor Microenvironment

The PDAC tumor microenvironment (TME) is composed of different cellular types, immersed in a very dense stroma which is the result of a desmoplastic reaction. It is a typical condition where stroma becomes highly fibrotic and creates a real barrier, contributing to isolate the cancer. Simultaneously, cancer-associated fibroblasts (CAFs), tumor-associated

macrophages (TAMs), and myeloid-derived suppressor cells (MDSCs) release inflammatory molecules and extracellular matrix (ECM) components, thereby reducing vascularization and increasing hypoxia. Unexpectedly, the effect of this hostile niche is tumor-promoting: cancer cells are "forced" to acquire more carcinogenic attributes and to reprogram themselves by actively interacting with surrounding cells. CAFs cover 15-85% of all the cellular lines that constitute the PDAC TME (11). Thus, many studies have focused their attention on their involvement in tumor progression, thereby finding several strategies through which they may act. First, the main work performed by CAFs is matrix deposition by secreting protein components such as glycosaminoglycans, collagens and fibronectin. (12). As a result, CAFs contribute to ECM fibrosis which in turn exacerbates the malignant tumor phenotype. Furthermore, CAFs have an important role in reprogramming the immune system through the production of the macrophage colony stimulating factor (M-CSF), a molecule responsible for pro-tumoral M2 macrophage activation (13). Indeed, even pancreatic stellate cells (PSCs) support the vitality of pancreatic cancer cells, providing them substrates for Krebs-cycle and via immune inactivation (14). Regarding the immune compartment, it is well known that the poor outcome of PDAC patients is related to a heavier involvement of tumor-promoting immune cells with tolerogenic functions over tumor-suppressive populations (e.g., CD8+ and CD4+ T cells, naïve B lymphocytes, monocytes, plasma cells, and activated mast cells) (15, 16). PDAC cells in fact have been found to attract M2-macrophages, neutrophils, T helper (Th17), regulatory B lymphocytes (B-reg), and myeloid-derived suppressor cells (MDSCs), thanks to the release of IL-1β, and to condition the remaining cellular microenvironment to suppress the activity of cytotoxic T cells (17). Altogether, these findings suggest a multitude of strategies through which PC can conditionate the TME.

2. Mitochondrial homeostasis: a hard affair

Usually defined as the "powerhouse of the cells", mitochondria play crucial roles within the cell, not only in energy production but also in several processes including cell death, fatty acid oxidation, innate immune signaling, etc. (18, 19). As the epicenter of many mechanisms, mitochondria are commonly exposed to stressful conditions that might affect their quantity and quality within the cytoplasm. Thus, cells developed an efficient mitochondrial quality control system to "safeguard" mitochondrial health (20).

2.1 Mitochondrial Quality Control System (MQC): the Guardian of Mitochondrial Safety

The mitochondrial quality control system (MQC) is based on three specific processes: mitochondrial dynamics, mitochondrial biogenesis and mitophagy. They cooperate to maintain mitochondrial homeostasis by clearing disrupted mitochondria, repairing mtDNA and generating new organelles. Mitochondrial dynamics act by shifting between fusion and fission to address moderate damage occurring within mitochondria (20). In this regard, Optic atrophy 1 (OPA1) and dynamin-like GTPase (DRP1) proteins are well-recognized as the main regulators of mitochondrial changes in shape and distribution. On the other hand, the remaining two processes are mostly involved in the control of the number and the size of mitochondria by coordinating transcription and replication of nuclear and mitochondrial genomes (mitochondrial biogenesis), and by ensuring the mitochondrial turnover through the elimination of unfunctional mitochondria (mitophagy). Disrupted mitochondria are specifically engulfed into autophagosomes and driven to lysosomes, allowing their degradation (21). By this way, the cell can reduce intracellular reactive oxygen species (ROS) and prevent cell death (22). This selective macro-autophagy can follow two different mechanisms: the ubiquitin/Parkin-dependent or the ubiquitin/Parkin-independent pathways. The first pathway is mediated by two main actors, PINK-1 and Parkin: under physiological conditions and when mitochondria are undamaged, PINK-1 is continuously

imported into the inner mitochondrial membrane (IMM) to be cleaved and then released into the cytoplasm to be degraded. In case of stressful conditions and in impaired mitochondria, the disruption of mitochondrial import channels prevents PINK-1 entrance which in turn localizes on the outer mitochondrial membrane (OMM) and recruits the E3 ubiquitin ligase Parkin. Here, PINK-1 phosphorylates and activates Parkin which will promote the ubiquitination of mitochondrial proteins through the ubiquitin-proteasome system (UPS) (23). In Parkin-independent process instead, the degradation of mitochondria is facilitated by BCL2 interacting protein 3 (BNIP3) and BCL2 interacting protein 3 like (BNIP3L). These mitophagy receptors are mainly activated under hypoxia (24). Thus, based on the entity of mitochondrial damage, the cell might selectively choose between these two alternatives.

2.2 Mitochondria-derived vesicles (MDVs): additional layers of mitochondrial quality check

In the setting of a mild stress, whether cells cannot afford the loss of mitochondria, they might also opt for packaging of mitochondrial components into microvesicles (25, 26). Studies suggest that their generation might be a first round of defense against mitochondrial damage that involves the selective removal of disrupted proteins instead of the entire mitochondria (27). First identified in 2008 by Neuspiel et al (28), mitochondrial-derived vesicles (MDVs) are shuttles of mitochondrial cargoes with diameters ranging from 70–150 nm. They appear as single-membrane vesicles when derived from the outer mitochondrial membrane (OMM) or in the form of double-membrane vesicles when derived from both the inner mitochondrial membrane (IMM) and the outer membrane. The MDV formation has been reported as a housekeeping process, occurring at low basal levels under homeostatic conditions and becoming upregulated in stressful environments. The PINK-1/Parkin activation is one of the main responsible for budding of oxidized membrane proteins and their consequent inclusion into vesicles (29). Interestingly, PINK-1 has been thought to act as a sensor of degree of mitochondrial damage, alternatively retrieving the actors of mitophagy or MDV biogenesis depending on the context. However, the downstream

players of the process are still lacking. MDVs can be distinguished based on the incorporation of two main proteins: TOMM20, an outer mitochondrial membrane protein necessary for importing nuclear-encoded proteins, and pyruvate dehydrogenase (PDH) subunits E2/E3bp located at the mitochondrial matrix (30). However, TOMM20+/PDH- MDVs appear mainly generated in response to extramitochondrial damage while the intramitochondrial oxidative stress usually causes the loading of mitochondrial matrix proteins into TOMM20-/PDH+ MDV populations (31). According to these findings, stress conditions altered the protein cargo of MDVs, which showed an enrichment of mitochondrial matrix and iron-binding proteins compared to baseline (31, 32). Furthermore, OPA-1 and SNX9 (Sorting Nexin 9) proteins have been recently reported to control the incorporation of both IMM and matrix proteins in the way that their silencing resulted in a reduction of matrix-positive MDVs (25, 30). As additional players of MQC system, MDVs are generally internalized by multi vesicular bodies (MVBs) to be finally disintegrated into the lysosomal compartment, thus allowing a rapid regulation of mitochondrial mass.

2.3 An alternative route for MDVs: the delivery into the extracellular space

Beyond the trafficking towards intracellular degradation systems, MDVs can pursue an alternative fate that drives them to the extracellular microenvironment in the shape of extracellular vesicles (EVs). EVs are heterogenous, phospholipid-enclosed structures generated by the cells and released into the extracellular space; they are often regarded as molecular fingerprints, acting as biomarkers that reflect the physiological state of their parental cells. Found to be involved in several mechanisms related especially to intercellular communication, EVs are classified by their size and content. This classification distinguishes *exosomes* (~30–150 nm in diameter) from *ectosomes* - which include microvesicles (~200–1000 nm) and large oncosomes (>1000 nm) (33). Recently, Zhou and colleagues used the term "mito-EVs" to define all EVs originating from mitochondrial structures (34). The delivery of MDVs as "mito-EVs" results from an alternative route of MVBs: instead of fusing with

lysosomes, they can interact with the plasma membrane causing its budding and the subsequent extracellular release of MVBs (30). Interestingly, rather than merely transporting mitochondrial debris out of the cell, "mito-EVs" appear to be generated to exert specific extracellular functions. For example, some studies have attributed a protective role to mito-EV-mediated crosstalk between donor and recipient cells, particularly in the context of cardiovascular diseases. Crewe *et al.* reported that the vesicular transmission of dysfunctional mitochondria from adipocytes to cardiomyocytes may act a protective preconditioning signal against myocardial injury (35). Similarly, the administration of "mito-EVs" to hypoxic cardiomyocytes has been shown to restore intracellular ATP levels and improve contractility (36). Recently, stressed brown adipocytes were found to specifically package PDH+/TOMM20-MDVs into extracellular vesicles through a Parkin-dependent mechanism (37). Thus, the impact of this organelle trafficking is strongly dependent on the functional state of mitochondria across the different cell types within the tissue.

3. Mitochondrial Dysfunction in Cancer: how does it manifest?

Although the initially accepted theory of the "Warburg effect" assigned a marginal role to mitochondria in tumor survival and progression, over the last few decades, mounting evidence has brought mitochondria *back to the forefront*, demonstrating the importance of a functional OXPHOS compartment for oncogenic potential. The dual impact on energy supply and cell death regulation revealed the critical role of mitochondria in the balance between the survival and apoptosis of cancer cells (38). Thus, the concept of metabolic reprogramming in tumors must involve both mitochondrial function and dysfunction. Indeed, changes in mitochondrial morphology, function, and dynamics are frequently correlated with tumor adaptation and progression. Here, we discuss the various ways through which mitochondrial dysfunction manifests, particularly within the tumorigenic context.

3.1 Defects of the mitochondrial TCA cycle and oxidative phosphorylation

Eukaryotic cells transform nutrients derived from the environment into available energy (ATP) via two main pathways: cytosolic glycolysis and oxidative phosphorylation (OXPHOS), which occurs within mitochondria. Under hypoxic conditions, glucose-derived pyruvate is transformed into lactate. In the presence of oxygen, instead, pyruvate is shuttled into the mitochondria and converted into acetyl-CoA to be oxidized through the tricarboxylic acid (TCA) cycle. This series of metabolic reactions leads to the reduction of NADH and FADH2, a critical step for subsequent oxidative phosphorylation. Consequently, the respiratory electron transport chain - embedded in the inner mitochondrial membrane and consisting of protein complexes (I to IV) - uses electrons derived from NADH and FADH2 to generate a proton gradient, which in turn drives ATP synthesis. Simultaneously, the crista junctions (CJs), by controlling ion movement, ensures distinct electrical potentials across the cristae and inner boundary membranes. In the context of cancer, however, functional dysregulations of the mitochondrial compartment are common; these can manifest as TCA cycle enzyme dysfunction, altered membrane potential, and reduced ATP levels (38). Moreover, genetic alterations of mitochondrial proteins are also responsible for inducing tumor growth and activating pro-survival signaling (39, 40), often involving key enzymes involved of the TCA cycle (41).

3.2 Generation of ROS

On the other hand, alteration of mitochondrial respiratory chain activity, frequently observed in cancer, can increase electron leakage, contributing to to the production of reactive oxygen species (ROS). Specifically, NADPH oxidase (NOX) has been reported to be activated by mitochondrial respiratory chain dysfunction, effectively promoting increased cellular ROS levels. Consequently, ROS generation is associated with genetic instability and can stimulate intensive cancer cell proliferation (41, 42).

3.3 Disruption of morphological integrity

Healthy mitochondria are characterized by intact membranes and tightly organized, well-defined cristae, which reflect a robust bioenergetic capacity (38). However, during tumor progression, mitochondria often undergo morphological shifts: they can appear swollen, enlarged, with disorganized cristae and dense matrices. Interestingly, these changes in mitochondrial shape correlate with specific metabolic features: cells exhibiting fragmented mitochondria tend to rely more on glycolysis than cells with predominant elongated mitochondria (43). Indeed, the outcomes of mitochondrial fragmentation and swelling are tissue-specific and depend on the degree of structural alteration. For example, mild swelling due to osmotic imbalances may still be compatible with mitochondrial function and metabolism (44), while non-physiological (pathological) swelling impairs the outer mitochondrial membrane and leads to cell death (45). In tumor tissues undergoing hypoxia, mitochondria can remain functional despite the enlarged morphology - albeit shifting toward a more glycolytic phenotype – thereby supporting rapid growth and providing protection against apoptosis. This survival strategy has been reported in ovarian, lung, and renal cancer as well as in osteosarcoma (46). On the other hand, tumors displaying early signs of apoptosis or necroptosis often exhibit markedly swollen and disrupted mitochondria, which are in turn associated with increased tumor aggressiveness (43).

3.4. mtDNA alterations

It is well established that mitochondrial dysfunction can be related to the nature of mtDNA. With its circular genome consisting of about 16.6 kb - encoding 13 proteins, 22 tRNAs and 2 ribosomal RNAs (rRNAs) - mtDNA is highly susceptible to mutations, which are usually found in a wide spectrum of human cancers (47). Recurrent mutations typically involve the D-loop region, protein-coding sequences, and rRNA or tRNA genes (48, 49). These most

commonly consist of point mutations and reduced copy numbers, although frame-shifting insertions and large-scale deletions have also been identified (41, 50). For instance, sequence analyses of tumor and normal tissue samples across five cancer types by The Cancer Genome Atlas (TCGA) revealed somatic mtDNA mutation frequencies of approximately 60% and 50% in rectal and colon adenocarcinomas, respectively, and around 30% in ovarian serous cystadenocarcinoma and acute myeloid leukemia, followed by 13% in glioblastoma (51). Alteration in mtDNA have also been associated with PDAC (52). Using an integrated approach of genomic, metabolomic, and phenotypic analysis on a cohort of patient-derived pancreatic cell lines, Hardie *et al.* found that most mtDNA mutations occurred within the protein-coding sites of the ND1, ND2, ND4, ND5, and ND6 subunits of Complex I. Furthermore, functional analysis revealed a more enhanced glycolytic activity alongside reduced OXPHOS (53). In a different study, nDNA and mtDNA were quantified in 43 PDAC tumor tissues and 31 normal adjacent pancreatic tissues by means of multiplex RT-PCR. Surprisingly, the authors observed a significant lower mtDNA copy number in PDAC samples compared to normal adjacent tissues (54). In fact, although the understanding of genotype-phenotype relationships remains limited, a new model of metabolic adaptation in PDAC is emerging, where the heterogeneous genomic landscape is proposed to converge on a common metabolic phenotype that in turn supports the occurrence of different mtDNA mutations (53).

3.5 Dysregulation of MQC

Mitochondrial dysfunction has been also correlated with the deregulation of mitochondrial quality control (MQC) mechanisms. Given their dynamic nature, mitochondria undergo constant changes through fission and fusion processes in response to metabolic demands. Mitochondrial dynamics thus maintain a balance that ensures stable organelle quality control. Consequently, the disruption of this equilibrium can reshape mitochondrial morphology and localization, inducing altered metabolic reprogramming (38, 55). For example, changes in the expression and function of key players such as OPA1 and

Mitofusins 1 and 2 (MFN1/2) have been reported in many types of cancer, when they act as critical modulators of the malignant phenotype (56, 57, 55). Furthermore, the failure to efficiently eliminate damaged mitochondria through mitophagy is a critical driver of cellular function impairment; the resulting accumulation of dysfunctional organelles can profoundly reprogram cell behavior. Conversely, in response to excessive pre-existing mitochondrial damage, mitophagy can be overstimulated, potentially driving the cell toward death due to its nature as a "self-eating" (autophagic) process. Interestingly, a new emerging role has been recently attributed to MDVs in tumor cells; they may compensate for impaired mitophagy, thereby supporting cancer adaptation by providing an alternative pathway for mitochondrial material disposal (58).

4. The ability of Pancreatic Cancer (PC) to drive the activity of mitochondria

As previously discussed, cancer can rearchitect tissue metabolic processes to fulfil novel energetic needs. In the context of PC, the typical cancer metabolism is heavily impacted by external and internal stimuli, involving both actors of the tumor microenvironment (TME) and several cellular pathways (59).

4.1 The role of the Tumor Microenvironment (TME) in PC

As discussed above, PDAC is characterized by a poorly vascularized and desmoplastic stroma, which results in hypoxia and nutrient deficiency. To cope with such hostile conditions, the adaptative response of cancer cells generally translates into a higher reliance on glycolysis for rapid ATP production, with a concomitant deficit in mitochondrial respiration. However, recent emerging metabolic studies in PC have revealed high plasticity between glycolysis and OXPHOS, proving that multiple neoplastic cellular subpopulations with different metabolic dependencies coexist and cooperate to foster a more aggressive tumor phenotype (60). Interestingly, Daemen *et al.* found an enrichment of three metabolic

pathways - glycolysis, lipogenesis and oxidative reduction - in PDAC (61). Simultaneously, since hypoxia imposes a significant nutrient restriction within the pancreatic tumor niche, additional strategies are adopted by PDAC cells to survive. For instance, they have been found to rely also on glutamine as a source of carbon and nitrogen (62), which can be shuttled into pancreatic cells even by means of exosomes derived from the TME itself (63). Olivares *et al.* additionally correlated the high collagen content of the extracellular matrix in PC with cancer survival, observing that tumor mitochondria were able to take up collagen fragments to compensate for nutrient deprivation (64). Thus, within such a hetero-cellular system where tumor and stromal cells reciprocally influence each other, there is a growing awareness of the benefits that a hybrid metabolic phenotype provides to PDAC aggressiveness compared to cells utilizing only a single pathway.

4.2 The contribution of mutated RAS proteins in respiratory injury of PC

Oncogenic KRAS is a well-established biomarker of PDAC and one of the most frequently activated tumorigenic drivers (65). Mutations in the GTPases HRAS, NRAS and KRAS have been recurrently detected in several human carcinomas. Basically, the RAS family modulates a variety of cellular responses linked to proliferation, survival and migration. Mutations occurring in these genes can dysregulate these pathways, contributing to cancer development (66). Among the existing mutation subtypes, the missense mutation G12D is the most common in PC. Interestingly, cells bearing oncogenic mutant KRAS usually exhibit compromised mitochondrial machinery: they tend to express a glycolytic phenotype combined with a defective mitochondrial respiratory chain and decreased oxidative flux through the TCA cycle (67). In PDAC cells, oncogenic KRAS drives this metabolic reprogramming: in response to the increased glucose demand, activated KRAS upregulates glucose transporter 1 (GLUT1) which in turn increases glucose uptake (68). Cancer cells consequently utilize more glucose-derived carbon for anabolic reactions such as the synthesis of ribose, amino acids, lipids, and glycosylation precursors. (68) Another hypothesized mechanism by which KRAS could cause mitochondrial dysfunction is linked

to KRAS protein translocation: Hu *et al*. postulated in the K-ras^{G12V}-expressing cells, the physical presence of KRAS protein within the mitochondria critically interferes with respiratory activity, by promoting the downregulation of NDUFAF1 (69). Together, these findings are gradually increasing the interest in filling the gaps in our knowledge regarding the real contribution of defective mitochondria to pancreatic cancer.

5. Horizontal Mitochondrial Transfer: a new emerging strategy for intercellular communication

The fate of fragmented mitochondria has been discussed at length: while, initially, their degradation was thought to be limited to the cytoplasm of the stressed cell through the mechanism of mitophagy, over time a new concept of cell survival has spread, whereby damaged mitochondria can undergo intercellular transfer (70). This results in the horizontal transfer of mitochondria, which occurs to aid the mitochondrial quality control system. This phenomenon may affect both damaged and healthy mitochondria depending on the metabolic needs of the tissue, but always requires a specific crosstalk between the donor and the recipient cells. Interestingly, there are different mechanisms through which this trafficking can occur (**Fig. 1**), including tunneling nanotubes (TNTs) or smaller carriers, such as extracellular vesicles (71). In some cases, even free mitochondria or mtDNA can be directly delivered. However, the real impact of intercellular mitochondrial transfer on both donor and recipient cells is still poorly characterized.

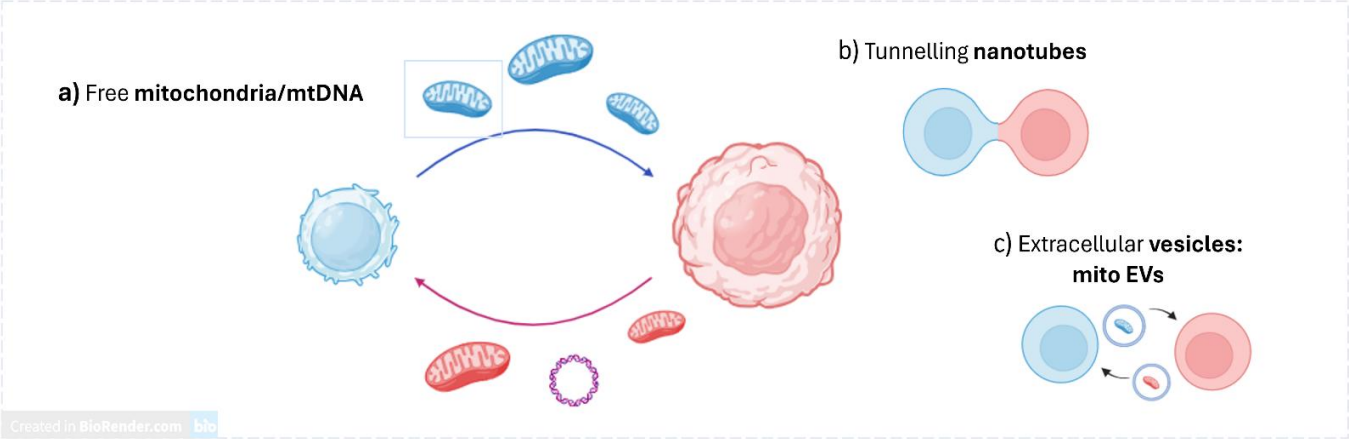


Figure 1. Different ways of horizontal mitochondrial transfer between cells.

5.1 The tendency of stressed cells to "outsource" the removal of dysfunctional mitochondria

When mitophagy mechanisms are dysregulated, an emerging compensatory response activated by cells is trans-mitophagy: they can commission the degradation of excess dysfunctional mitochondria to recipient cells (72) In this way, the donor cell is able to maintain mitochondrial homeostasis. For example, the trafficking of damaged mitochondria has been reported from retinal ganglion cells to adjacent astrocytes (73). Indeed, as mentioned above, Ikeda *et al*. (36) demonstrated that the release of "mito-EVs" by stem cell-derived cardiomyocytes restored the intracellular bioenergetics of the ischemic myocardium. Interestingly, in the context of cancer, many studies are gradually exploring a new way of communication between tumor and stromal cells involving mitochondria: in the work of Valdebenito and colleagues, TNTs induced by oxidative stress mediated the long-range exchange between glioblastoma and primary astrocytes, allowing the transfer of enlarged and metabolically altered mitochondria from cancer cells into neighboring primary astrocytes (74). Similarly, tunnelling nanotubes promoting trans-mitophagy have been recently observed connecting multiple myeloma cell with BM stromal cells (BMSCs), a process that correlates with cancer survival (75).

5.2 The contribution of neighboring cells in providing healthy mitochondria

Mitochondrial exchange does not exclusively consist of the unidirectional transport of damaged material. Rather, it is a mechanism through which cells within the microenvironment can actively participate in the overall homeostasis of the tissue. Thus, this delivery can also involve functional mitochondria which in turn may help to stabilize the bioenergetic potential of the target cell. The transfer of intact mitochondria is a recurrent phenomenon in glioblastoma, associated with tumorigenesis: mitochondria are shuttled from astrocytes to cancer cells, where they participate in the upregulation some metabolic pathways involved in the proliferative potential (76). Indeed, the intercellular transfer of mitochondria has been reported to have additionally a pro-metastatic role: Zhang *et al.* recently found that the uptake of platelet-derived healthy mitochondria by osteosarcoma cells enhanced their capacity to metastasize to the lung (77). Thus, given the frequency of this phenomenon especially in pathological conditions, mitochondrial transfer merits more attention from researchers.

5.3 Circulating cell-free mtDNA (cf-mtDNA)

Cells experiencing mitochondrial stress are usually prone to releasing mitochondrial damage-associated molecular patterns (DAMPs) which in turn contribute to the prompt regulation of the surrounding inflammation. Among DAMPs, cell-free mtDNA can be released into the extracellular milieu. Cases of mtDNA leakage have been recently reported in different human diseases, including cancer, where interestingly they play crucial roles in reprogramming the tumor microenvironment. For example, the emergence of resistance to Sorafenib in hepatocellular carcinoma (HCC) was correlated with an increase in circulating cell-free mtDNA derived from neoplastic cells (78); interestingly, Sorafenib induced mitochondrial dysfunction and promoted the release of mtDNA into the extracellular matrix of HCC. Once released, the genetic material was taken up by tumor-associated macrophages (TAMs), where it promoted M2 phenotype polarization, thereby supporting

cancer progression (78). The leakage of mtDNA is strictly dependent on morphological changes of mitochondrial cristae: any type of structural disarray involving cristae might increase mitochondrial membrane permeability and promote the clustering of mtDNA, thus facilitating its subsequent release (79). Other conditions that drive this phenomenon are generally linked to dysregulated mitophagy, altered mitochondrial dynamics and programmed cell death. Furthermore, the release of mtDNA from donor cells and its exchange with recipient cells can be also facilitated by extracellular vesicles. This type of transfer has been reported in tissue repair, immune regulation and pathological events (80). Together these data confirm that circulating cell-free mtDNA is becoming established as a promising biomarker for cancer diagnosis and monitoring (81).

6. Recent Findings and Aim of the Study

6.1 New Insights into the Clear Cell Carcinoma of the Pancreas (CCCP)

Because of diverse histopathological features, several PDAC variants exist, among which the "clear-cell" variant is one of the least defined. First identified in 1980 (82), clear-cell carcinoma of the pancreas (CCCP) has been reported as a rare morphological pattern of PDAC associated with poor patient outcomes (83) and where a relevant fraction of neoplastic cells exhibits a characteristic clear cytoplasm, conferring a "foamy" appearance to the tissue (**Fig. 2A**). Since no previous study has deeply investigated the determinants of CCCP differentiation in terms of ultrastructure, we recently applied transmission electron microscopy (TEM) to visualize a CCCP surgical specimen from 65-year-old patient (84). After confirming that the "clear" aspect was not due to the accumulation of mucin vacuoles, we performed a TEM characterization and, surprisingly, found swollen electron-lucent mitochondria undergoing a loss of structural integrity (**Fig. 2B**). Consistent with these observations, the detection of NADH dehydrogenase [ubiquinone] 1 alpha subcomplex, 4-like 2 (NDUFA4L2) expression on the whole tissue slice confirmed the altered functional

state of clear-cells mitochondria compared to non-tumoral areas. More interestingly, we captured membrane-mediated release of these electron-lucent structures in the extracellular space (**Fig. 2C**). These findings strongly suggested a possible vesicular exchange among cells that might involve dysfunctional mitochondria.

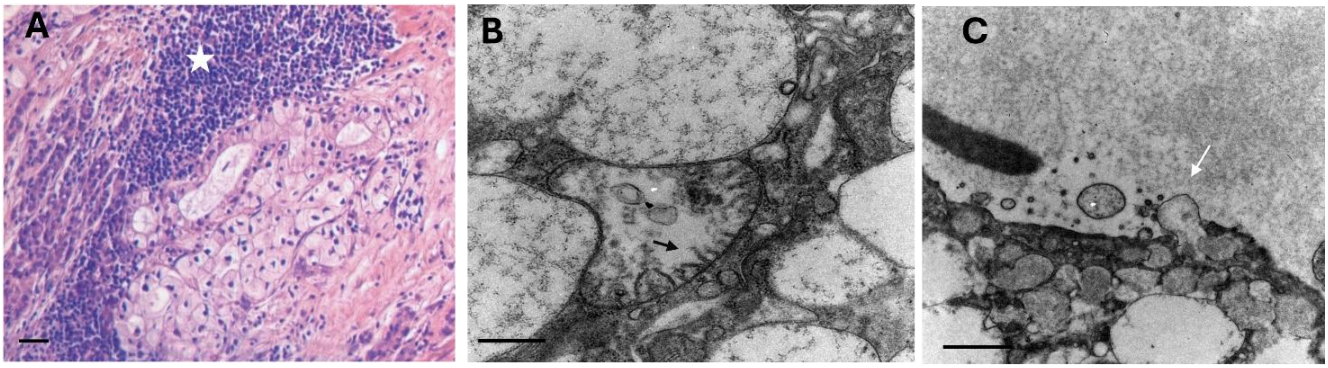


Figure 2. Histochemical and ultrastructural characterization of a CCCP surgical specimen. (A) Nest of "foamy" tumor cells immersed in a typical desmoplastic reaction (white star). Magnification: 10×. (B) Clear cells showed recurrent fragments resembling damaged mitochondrial cristae (black arrow) (20,000×; scale bar: 0.5 μm) (C). The formation of an electron-lucent vacuole from the plasma membrane is indicated by the white arrow (12,000×; scale bar: 1 μm).

6.2 Aim of the Study

Since we previously suggested an interesting connection between mitochondrial dysfunction and the progression of a rare histological subtype of PDAC, the CCCP variant, that could imply the release of extracellular vesicles carrying mitochondrial cargo in the extracellular space (84), we hypothesized that these signs of metabolic reprogramming could also be present in conventional PDACs and correlate with patient diagnosis and prognosis. Thus, the aim of this study is to establish a preclinical proof-of-concept that the intercellular transport of dysfunctional mitochondria, mediated by EVs, could represent a

new parameter for stratifying PDAC sub-populations. Notably, the proteomic characterization of small extracellular vesicles secreted by human pancreatic cancer cell lines has showed a significant enrichment for proteins involved in vesicle formation and secretion pathways, as well as proteins associated with metabolic processes (85). However, given our focus on mitochondria, a more specific comparative analysis - aimed at investigating and quantifying the enrichment of mitochondrial cargo in normal versus tumor-derived vesicles - is critically needed.

7. Materials and Methods

7.1 Human Cell Cultures

Human pancreatic cancer cell lines BXPC-3 and PANC-1 were purchased from the American Type Culture Collection (ATCC, Manassas, VA). The HPDE cell line, the immortalized human pancreatic duct epithelial cell line, was generously provided by Prof. Trerotola's Laboratory (Center of Advanced Studies and Technology, Chieti, Italy). BXPC-3 cells were cultured in RPMI 1640 Medium with L-Glutamine (Sial, Rome, Italy), while PANC-1 cells were maintained in High Glucose Dulbecco's modified Eagle's medium (DMEM) (Sial, Rome, Italy). Both media were supplemented with 10% (v/v) fetal bovine serum (FBS) and a 1% (v/v) antibiotic solution (Penicillin-Streptomycin) (Sial, Rome, Italy). HPDE cells were maintained in Keratinocyte Serum-Free Medium (KSFM) (Thermo Fisher Scientific, USA) enriched with KSFM supplements, including Epidermal Growth Factor (EGF) and bovine pituitary extract (BPE), added at the time of use (Thermo Fisher Scientific, USA). Each cell line was tested and confirmed to be free from mycoplasma. All the cell lines were cultured at 37° in a humidified atmosphere with 5% CO_2.

7.2 Extracellular Acidification Rate (ECAR) and Oxygen Consumption Rate (OCR)

Quantification of mitochondrial respiration and glycolysis was performed by measuring the oxygen consumption rate (OCR) and extracellular acidification rate (ECAR) in living cells, utilizing a Seahorse XF24 Extracellular Flux Analyzer (86). On day 1, cells from the control (HPDE) and pancreatic cancer cell lines (PANC-1, BXPC-3) were plated at a density of 1.5–5 × 10^4 cells per well in 100 μL of growth medium per well in XF24 cell culture plates and maintained at 37°C for 12-18 h. Subsequently, the sensory cartridge was hydrated by filling each well of the utility plate with 1 mL of Seahorse XF Calibrant and left at 37 °C in a CO_2-free incubator overnight. On the day of the assay, cells were incubated with replaced Seahorse assay medium at 37°C in a CO_2-free incubator for 1 h. During the incubation, the XF Cell Stress Test Compounds for both the OCR and ECAR assays were prepared and loaded in the hydrated sensory cartridge, following the recommended concentrations: oligomycin (2 μg/mL), FCCP (300 nM), antimycin A (1 μM), glucose (5 mM), Oligomycin (2 μg/mL) and 2-deoxy-D-glucose (2-DG) (40 mM). After the completion of the Seahorse XF24 run, cells were lysed directly on plate for protein quantification the day after using the Pierce BCA Protein assay Kit (Thermo Fisher) to normalize the OCR and ECAR plots.

7.3 3D human patient-derived Organoid (PDO) Culture

Established PDAC patient-derived organoid cell lines were generously provided by Prof. Reichert's Laboratory (Translational Pancreatic Cancer Research Center, Munich, Germany) and cultured in 24-well plates as domes, formed by mixing cells with Matrigel (30 μL/well). After the solidification of the Matrigel, 500 μL of warm PDO culture medium was added to each well. The complete composition of the PDO culture medium have been previously reported (87). Each PDO cell line was tested and confirmed to be free from mycoplasma and maintained at 37° C in a humidified atmosphere with 5% CO_2. For drug tests, PDOs were treated with 10 μM MRTX1133 by first removing the organoid growth medium and then replacing it with 500 μL of drug-containing culture medium. After six hours of incubation

at 37° C in a humidified atmosphere with 5% CO_2, PDOs were harvested for subsequent analyses.

7.4 Gene-set-enrichment analysis (GSEA)

To screen for differentially expressed genes among PDO subpopulations, a Gene Set Enrichment Analysis (GSEA) was performed on RNA-seq count data, drawing from the PDO-derived RNA-seq databank of Reichert's Lab. Gene sets were retrieved from the Molecular Signatures Database (MSigDB).

7.5 ATP and Oligomycin/2DG Dose-Response Growth Measurements

Changes in cellular ATP concentrations in 3-dimensional organoid cell cultures were measured using the Cell Titer-Glo assay, based on previous studies (88). To generate oligomycin and 2-deoxy-D-glucose (2-DG) dose-response curves, 1×10^3 cells in 100 µl /well were plated in triplicates for each condition in 96-well plates and treated with oligomycin (100 ng/ml) or 2-DG (10 mM) for 6 hours of treatment. The dose-response curves were generated by assaying cells with CellTiter-Glo reagent (Promega) at every two hours (from t = 0 to t = 6 h) and then plotted using GraphPad Prism (GraphPad Software).

7.6 Immunofluorescence Assay

Between 5 and 10×10^3 cells of each PDO cell line (untreated or treated with MRTXX1133) were grown on Ibidi slides and fixed with 4% of paraformaldehyde (PFA) (15 min, RT). After permeabilization in 0.2% Triton X-100 (10 min, RT) and blocking in 0.1% BSA (overnight at 4°C), cells were incubated with a 1:100 dilution of anti-PINK1 (Polyclonal Antibody, Rabbit, 23274-1-AP, Proteintech) and anti-PDH (Pyruvate Dehydrogenase Antibody Cocktail, Mouse, 45-6799, Thermo Fisher) primary antibodies overnight at 4°C under gentle agitation. This was followed by incubation with a 1:250 dilution of Alexa Fluor 488 goat anti-mouse

and Alexa Fluor 594 donkey anti-rabbit secondary antibodies. Stained organoids were visualized under the Leica SP8 Confocal/Multiphoton Microscope, located at the Technical University of Munich (TUM).

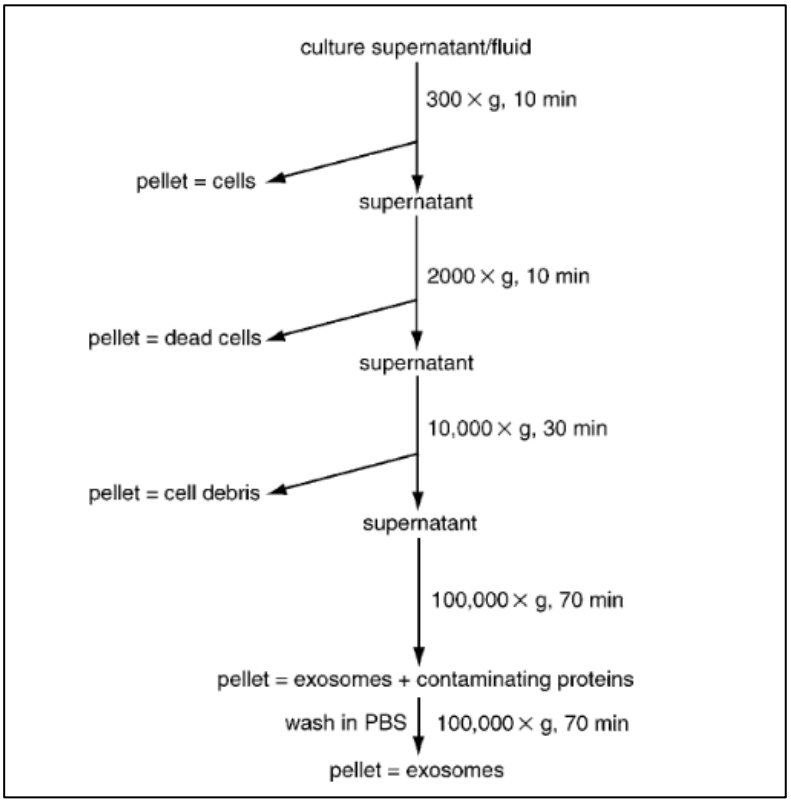
7.7 Transmission Electron Microscopy (TEM)

For ultrastructural evaluation, human PDAC organoids and two-dimensional pancreatic cancer cells were fixed in a solution of 3 % glutaraldehyde (Electron Microscopy Sciences, Hatfield, PA, USA) and 0.1 M cacodylate buffer (Electron Microscopy Sciences) (pH 7.2–7.4) for 2 h at 4 °C and post-fixed in 1% osmium tetroxide (Electron Microscopy Sciences) for 1 h at 4 °C. After washing in cacodylate buffer, samples were dehydrated in an ascending series of acetone solutions (40%, 60%, and 100%) and finally embedded in Epon resin (Electron Microscopy Sciences). Semi-thin sections (about 800 nm thick) were obtained using a Reichert ultramicrotome (Reichert, Depew, NY, USA), and then stained with toluidine blue for observation by light microscopy. Subsequently, ultrathin sections (70 nm) were cut and mounted on 200-mesh copper grids (Electron Microscopy Sciences) to be counterstained with UranyLess and lead citrate staining solutions (Electron Microscopy Sciences). Jeol JEM SX100 electron microscope was used for sample visualization.

7.8 Collection of cell-conditioned media and purification of EVs

EVs were isolated from cells using the ultracentrifugation protocol previously described by Thery *et al*. (89). All cell lines were grown in sixteen T75 cm^3 flasks until they reached ~80% confluency to collect a final supernatant (s/n) of ~240 mL of conditioned medium. After the first collection of the s/n, fresh medium was added to allow a second collection after 24h. Subsequently, cells were detached, counted and re-plated into new sixteen new T75 cm^3 flasks. A third collection of s/n was performed thereby obtaining three final EVs pellets derived from the same cell line. This operation has been performed for all the cell lines. The extraction protocol, as shown in the flow chart below, is as follows: the conditioned medium

was centrifuged at 2000 g for 10 min to remove dead cells and transferred to polypropylene tubes (Beckman Coulter, USA). Tubes were balanced with sterile PBS 1x w/o $CaCl_2$/$MgCl_2$ and ultracentrifuged at 10,000 g for 30 min, at 10°C using a fixed-angle rotor SW28 (Beckman, k-Factor = 246) to remove floating debris. Enrichment of EVs was carried out by ultracentrifugation at 100,000 g for 3 h, at 10 °C using the same rotor. The EV pellets were resuspended in PBS and then concentrated using a SW 41 Ti swinging-bucket (Beckman, k-Factor = 124) at 100,000 g, for 90 min, at 10 °C. The s/n was removed and the EVs pellets were flash frozen first in liquid nitrogen and stored at -80°C until their application. Final EV pellets were validated through characterization via qRT-PCR.



Flowchart of the extracellular vesicle purification process by Raposo et al. (90)

7.9. mtDNA Quantification

Total genomic DNA was isolated using a Genomic DNA Purification Kit (Promega). Real-time quantitative PCR (RT-qPCR) was performed using Fast SYBR Green PCR Master Mix

(Applied Biosystems). Human β2m forward (5′-TGCTGTCTCCATGTTTGATGTATC T-3′) and β2m reverse (5′-TCTCTGCTCCCC ACCTCTAAGT -3′) or tRNA-Leu(UUR) forward (5′-CACCCAAGAACAGGGTTTGT—3′) and tRNA- Leu(UUR) reverse (5′-TGGCCATGGGTATGTTGTTA-3′) primers were used (91). All results were normalized to the human housekeeping genes β-actin and TATA-box binding protein (TBP).

7.1.1 Flow Cytometry analysis of extracellular vesicles

For each sample, 100 μL of supernatant was stained with a membrane dye (LCD: lipophilic cationic dye) and incubated for 45 minutes at room temperature in the dark, as previously reported (92). Samples subsequently underwent fixation and permeabilization using Cytofix/Cytoperm (BD Biosciences, La Jolla, CA, USA) and were then labeled with the primary antibodies listed in Table 1. After 30 minutes of incubation, samples were stained with the corresponding fluorescent secondary antibodies (Table 1) (92). Following a 30-min incubation in the dark, at least 500 μL of 1× PBS was added to each tube, and 3 x 10^3 events *per* sample were acquired using a FACSymphony A5 flow cytometer (BD Biosciences, La Jolla, CA, USA). Sample dilution was optimized to avoid coincidence (swarming) effects. The trigger threshold was set on the APC channel (LCD emission channel), and bi-exponential scaling and height (H) signals were used for all parameters. All reagents were titrated under assay conditions (93). Instrument performance, data reproducibility, and fluorescence calibration were monitored, and fluorescence minus one (FMO) controls were used to establish background signals, as recommended (94, 95, 96, 97).

Table 1. Flow Cytometry Reagent List			
Surface Stainings	**Amount per test**	**Manufacturer**	**Catalogue #**
LCD	1 µl	BD	564697
Intracellular Staining	**Amount per test**	**Manufacturer**	**Catalogue #**
TOMM20 Polyclonal antibody	1:2500	Proteintech	11802-1-AP
NDUFA4L2 Polyclonal antibody	1:500	Proteintech	16480-1-AP
Secondary Antibody	**Amount per test**	**Manufacturer**	**Catalogue #**
Anti Rabbit IgG Alexa Fluor Plus 405	1 µl	Invitrogen	A48254
Anti Mouse IgG Alexa Fluor Plus 546	1 µl	Invitrogen	A11018
LCD= lyphopilic cationic dye.			

8. Results

8.1 Human Pancreatic Cancer Cell Lines differently reprogram their energetic metabolism.

We initially selected two pancreatic cancer cell lines, PANC-1 and BXPC-3, based on their differing levels of cell adhesion, migratory capacity, and tumorigenicity (98). Additional functional analyses have previously shown distinct metabolic profiles, attributing a more glycolytic phenotype to BXPC-3 (99). For further confirmation, we investigated any cellular ATP changes after treatment with 2-Deoxyglucose (2-DG) and oligomycin (Oligo) inhibitors, commonly used to mimic the suppression of glycolysis and OXPHOS, respectively (**Fig. 3A**). Our data showed that the ATP content decreased in a glycolysis-dependent manner in both cell lines, although BXPC-3 cells were more sensitive to 2-Deoxyglucose exposure. Compared to the OXPHOS inhibitor, 2DG was more efficient in depleting the cellular ATP content during the same time of incubation.

However, to assess the actual metabolic state of the cells, we evaluated glycolitic lactate production and mitochondrial oxygen-consumption by means of a Seahorse Extracellular

Flux (XF) analyzer, a highly sensitive tool that provides *real-time* metabolic profiles of both mitochondrial respiration and glycolysis (100). As shown in the Oxygen Consumption Rate (OCR) and Extra-Cellular Acidification Rate (ECAR) plots (**Fig. 3B**), PANC-1 is the most respiratory cancer cell line while BXPC-3 appears mainly glycolytic. The healthy control (HPDE), by contrast, shows the lowest overall metabolic activity.

Notably, these data were consistent with previous results (99) and with our subsequent TEM observations. By exploring the ultrastructure of each cell line, we noticed different mitochondria morphologies reflecting their functional state: while in HPDE cells, mitochondria appeared mostly preserved in their morphological integrity with a typical elongated shape, we found different scenarios in cancer cells, where both BXPC-3 and PANC-1 were affected by mitochondrial damage (**Fig. 3B**). Notably, BXPC-3 showed later stages of degeneration, resulting in the appearance of swollen and round mitochondria. In contrast, PANC-1 cells exhibited partially disrupted mitochondria, typically displaying early stages of morphological alteration, including the enlargement of cristae.

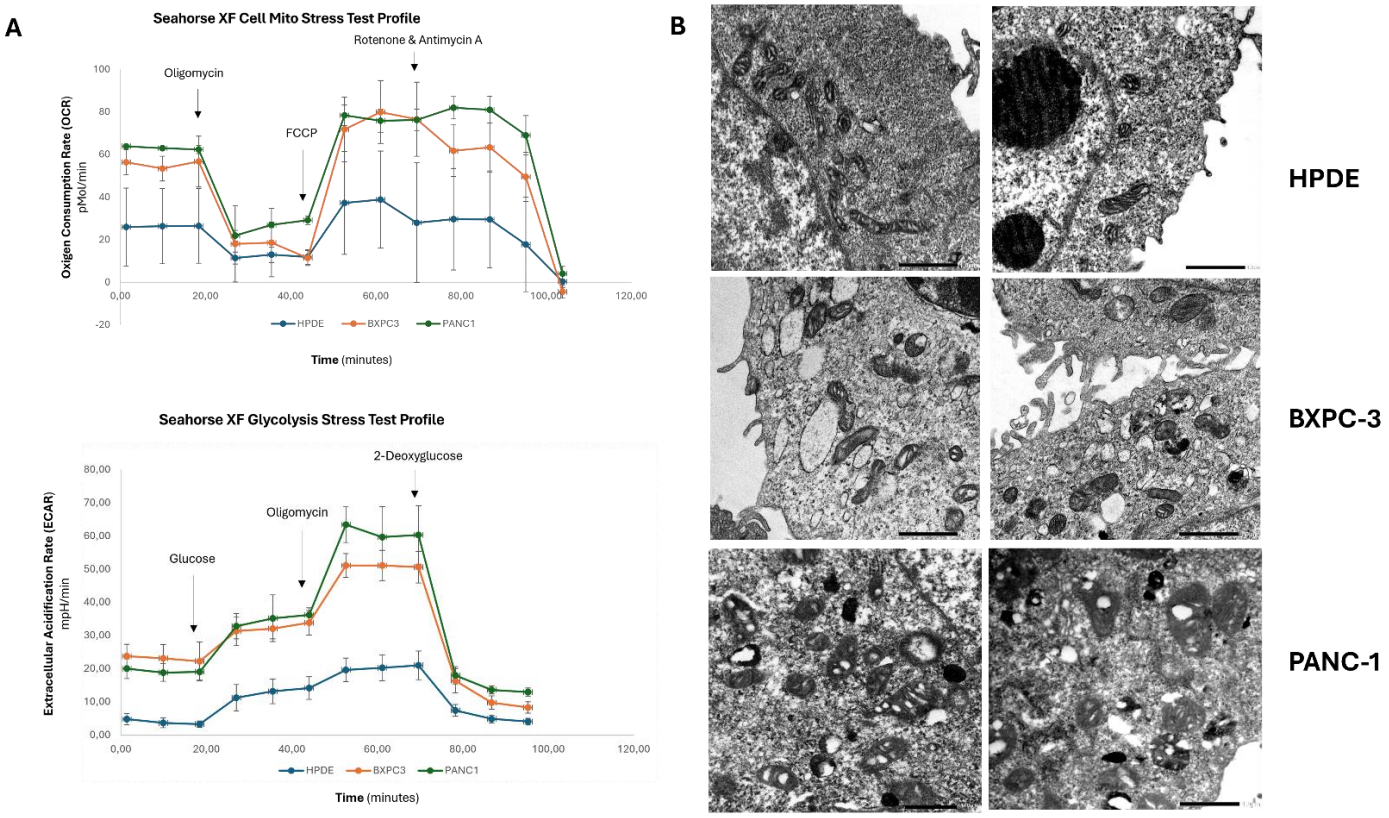


Figure 3. Metabolic Characterization of Pancreatic 2D cell models. (**A**) OCR (above) and ECAR (below) plots showed the stratification of pancreatic cell lines into 3 metabolic groups. (**B**) TEM visualization of mitochondria in HPDE, BXPC-3 and PANC-1 cell lines (8,000×; scale bar 1 μm).

Notably, BXPC-3 cells exhibited a higher abundance of autophagosomal structures, indicative of the efficient clearance of dysfunctional mitochondria. Conversely, PANC-1 cells showed numerous multivesicular bodies (MVBs) in the extracellular space, predominantly localized near the plasma membrane, suggesting enhanced secretory activity (**Fig. 4**).

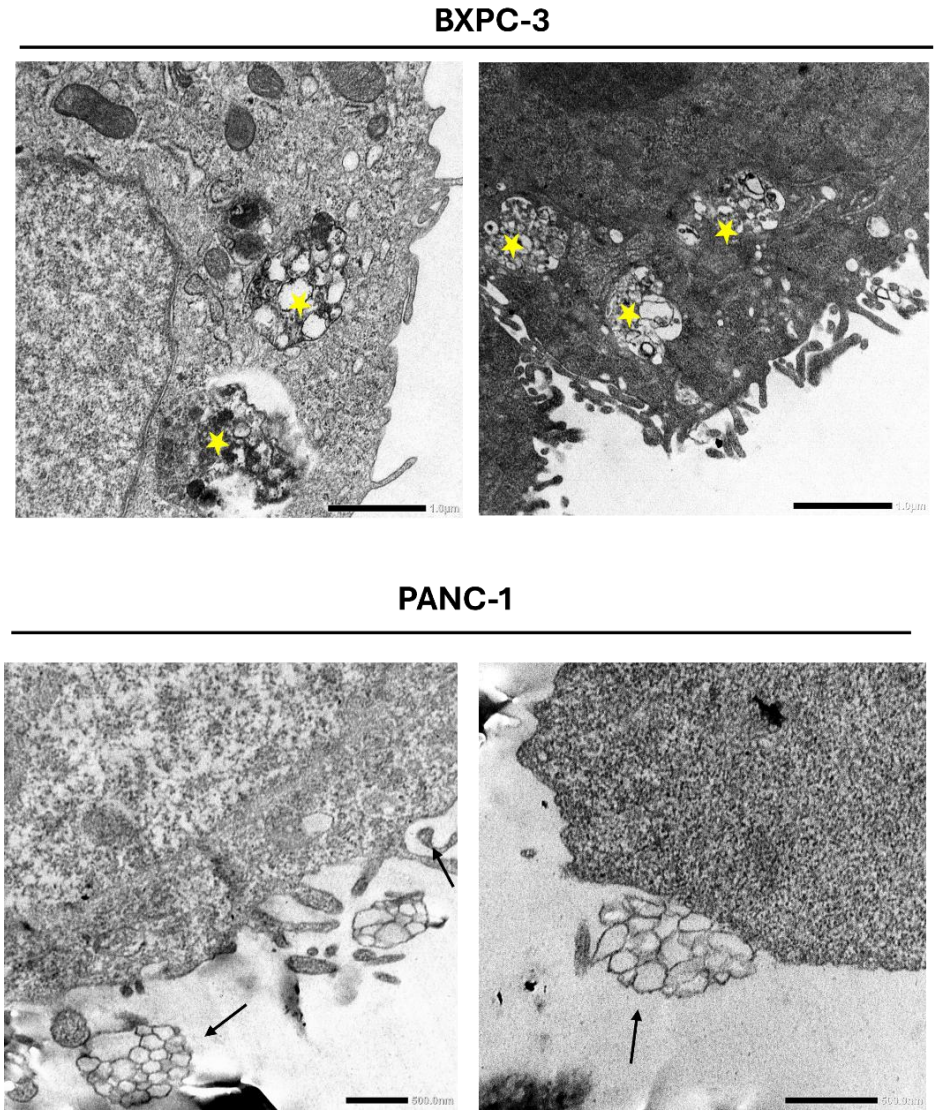


Figure 4. Distinct autophagic and secretory profiles in BXPC-3 and PANC-1 cells, respectively. Autophagosomal structures are marked with yellow stars (8,000×; scale bar 1 μm). Black arrows indicate multiple multivesicular bodies in the extracellular space (15,000×; scale bar 0.5 μm).

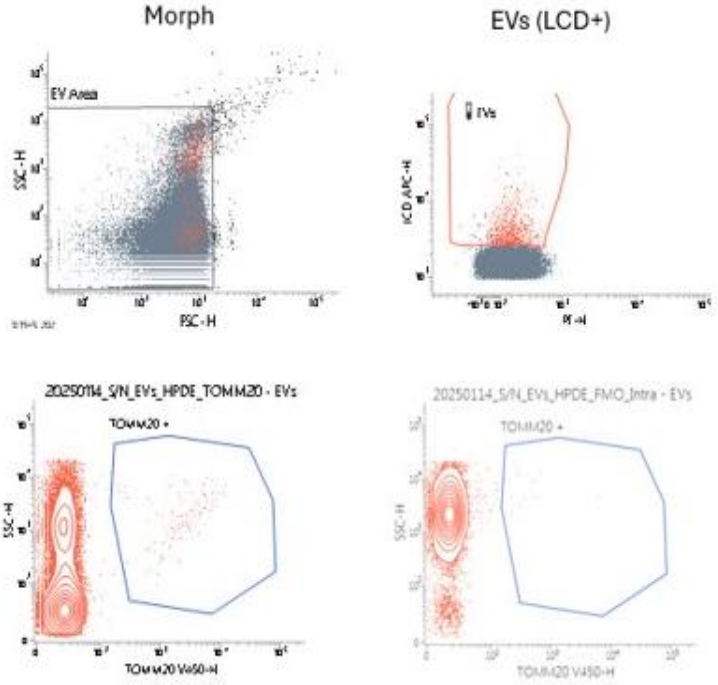
8.2 Comparative analysis of EV secretomes highlights increased mitochondrial EVs in PDAC cells

We next investigated potential differences within cell-derived secretome. First, we collected and screened the cell culture supernatants for EV production and for the presence of mitochondrial surface markers via flow cytometry (FACs). Subsequently, we performed real-time PCR on extracellular vesicles isolated by ultracentrifugation to quantify the amount of mtDNA. By combining these two methods, we were able to characterize the mitochondria-derived EVs (mito-EVs) within the cell secretome.

For the first objective, an optimized protocol (92) allowed us to separate, count and classify EVs. The dot plots below show the gating strategy used: EVs were selected from the platelet-free area by size (FSC/SSC) and by their positivity for a lipophilic cationic dye (LCD) (**Fig. 5**). Once the EV compartment was gated, we evaluated the expression of TOMM20, a member of the translocase of the outer mitochondrial membrane (TOM) complex. Preliminary data showed that vesicles derived from the conditioned media of tumor cell lines were richer in mitochondrial marker expression compared to those derived from the healthy control (HPDE). Notably, a higher production of mitochondria-derived vesicles was observed in PANC-1 cells.

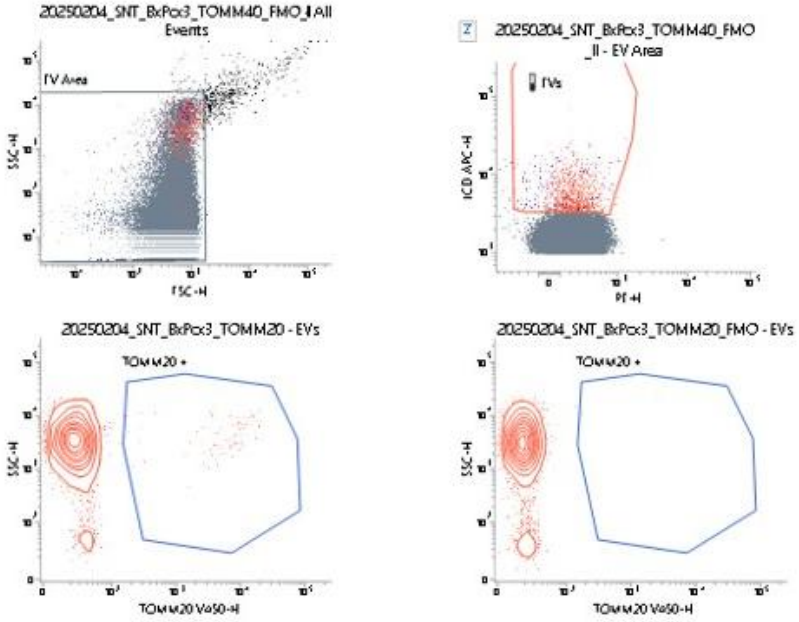
HPDE

%TOMM20_EVs	1.19



BXPC-3

%TOMM20_EVs	2.23



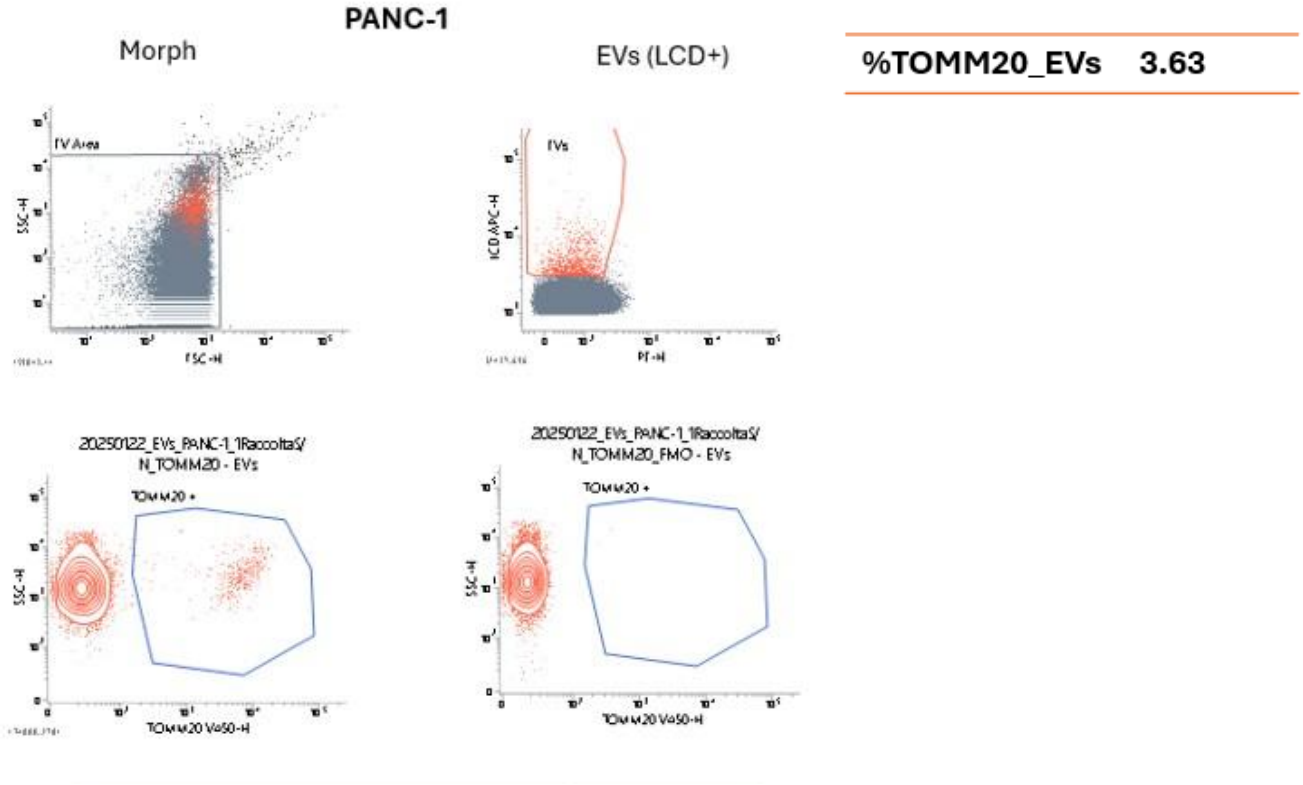


Figure 5. Optimized EV separation and classification of mitochondrial-derived EVs (mito-EVs) content in cell-conditioned media. The tables report the percentage of TOMM20-positive EVs compared with the percentage of EVs detected in the FMO (Fluorescence Minus One) control.

For the second purpose, we isolated EVs using the ultracentrifugation protocol (90). The EV-derived pellet was subjected to DNA extraction to detect the presence of mtDNA. In line with our previous findings, mitochondrial DNA was detected in vesicles from all three cell lines, with higher levels in those derived from tumor cells. RT-qPCR analysis also revealed a higher relative amount of mitochondrial genetic material in PANC-1-derived vesicles. Although preliminary, these results are consistent with our earlier observations obtained via transmission electron microscopy.

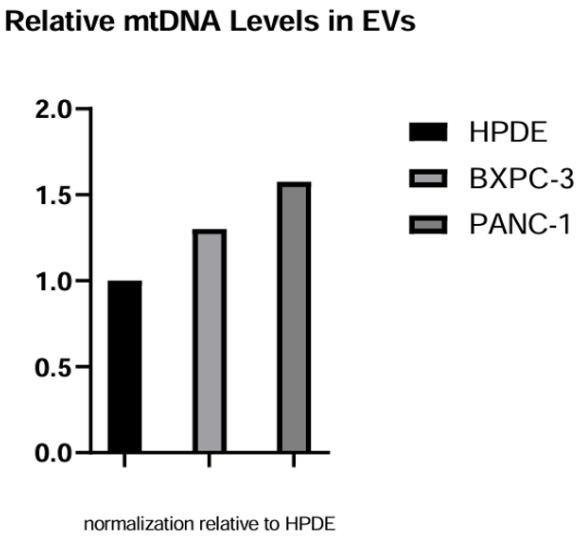


Figure 6. Relative mtDNA levels detected in extracellular vesicles derived from HPDE, BXPC-3, and PANC-1 cell lines. A trend toward higher mtDNA content is observed in vesicles from tumor cells. Data are shown as relative values normalized to HPDE.

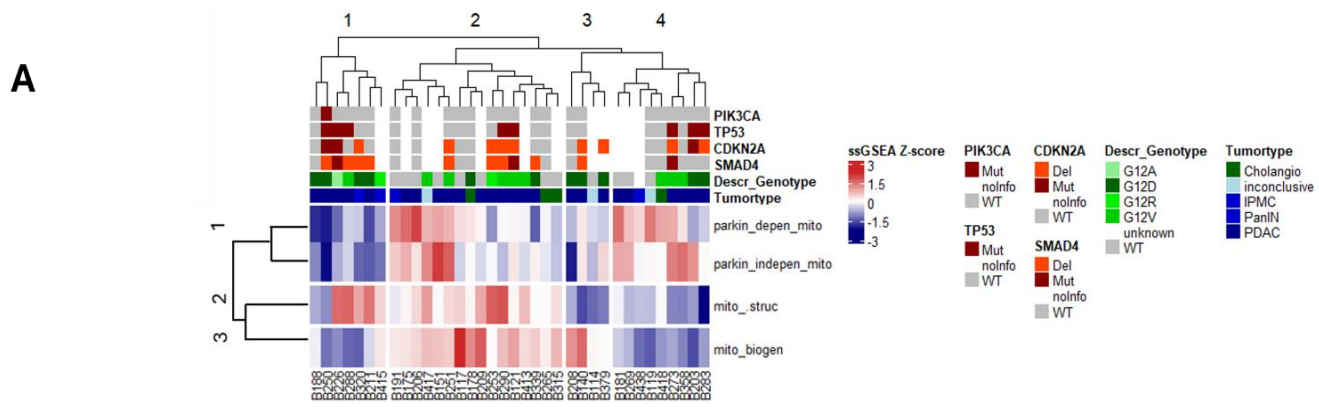
8.3 Patient-Derived Organoids (PDOs) can mitigate the elimination of mitochondria

Using pancreatic cancer cell lines as a proof of principle, we explored the possibility of translating the study to patient-derived organoids (PDOs). Given their more complex structural organization, organoids provide a new level of communication that might influence the quantity and composition of secreted extracellular vesicles. Thus, we addressed this hypothesis by identifying differences or commonalities between EVs derived from cancer cells growing in 2D versus those derived from 3D cultures.

Initially, we sought a starting point by linking cellular mitochondrial alterations to the presence of mitochondrial material in the secretome. Thus, given that mitochondrial homeostasis and content result from a fine-tuned equilibrium between mitogenesis and the selective elimination of damaged mitochondria via mitophagy (101), we screened PDO-derived RNA-seq data from the corresponding patients for potential modulation of these pathways. We also included genes responsible for maintaining morphological integrity such as OPA1 and TOMM70.

Notably, Gene Set Enrichment Analysis (GSEA) revealed an interesting clustering of the cases, categorizing the PDOs into four subgroups (**Fig. 7A**). We also observed a marked tendency toward the downregulation of genes involved in mitochondrial degradation. In light of the contradictory role of mitophagy described in the literature - whereby it can function as either a tumor suppressor or a tumor promoter depending on the tumor stage - we sought to determine whether differences exist in the mitochondrial component of the secretome derived from established tumors compared with preneoplastic lesions exhibiting contrasting mitophagy signatures.

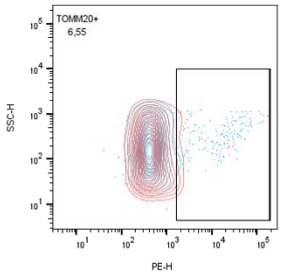
To this end, we analyzed EV-associated mitochondrial markers with distinct localizations: TOMM20 (an outer mitochondrial membrane protein), and NDUFA4L2 (an inner mitochondrial membrane component) (**Fig. 7B**). Interestingly, our results revealed that EVs from all conditions were positive for both markers, confirming the presence of a mitochondrial component in the secretome. However, the proportion of NDUFA4L2-positive EVs varied across samples, being higher in secretomes derived from established tumors with suppressed mitophagy (e.g. B250, B211) and lower in preneoplastic conditions with enhanced mitophagy (B191). Overall, these data support the idea that the downregulation of mitophagy might favor the extracellular release of mitochondrial components, reflecting a potential adaptation to mitochondrial impairment.

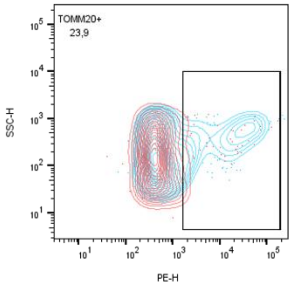


B

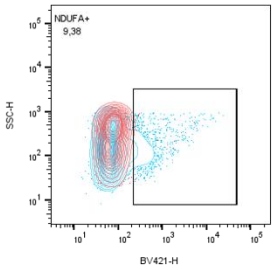
B250 (- mitophagy; G12D KRAS mut, **PDAC**)

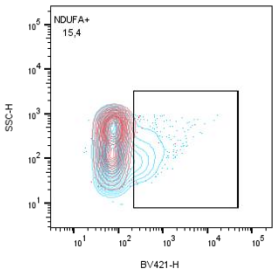
TOMM20





NDUFA4L2



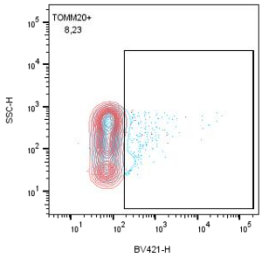


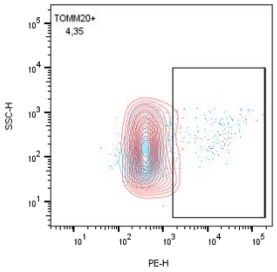
% mean EVs **TOMM20** + = **15.23 %**

% mean EVs **NDUFA4L2** + = **12.39 %**

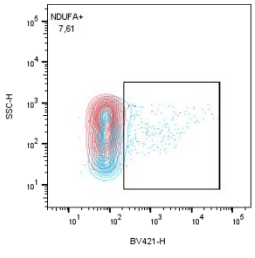
B211 (- mitophagy; G12D KRAS mut, **PDAC**)

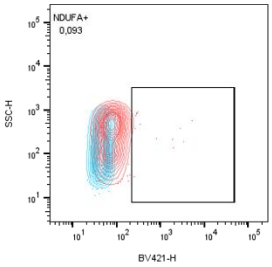
TOMM20





NDUFA4L2





% mean EVs **TOMM20** + = **6.29 %**

% mean EVs **NDUFA4L2** + = **3.56 %**

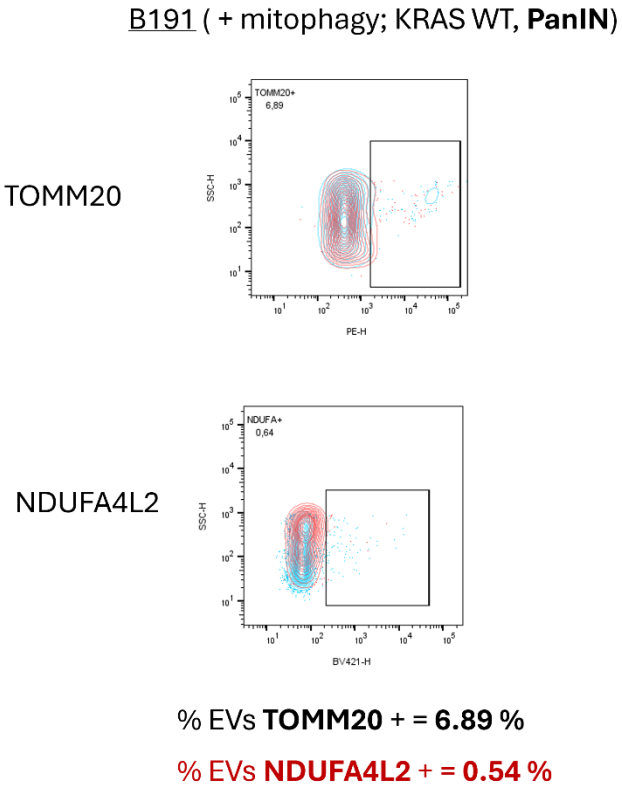


Figure 7. (**A**) Selection of Patient-Derived Organoids according to altered mitochondrial homeostasis signatures. The heat map shows the stratification of PDOs following GSEA of RNA-seq data. Regarding mitophagy, two distinct gene sets were used, referencing two existing pathways: Parkin-dependent and Parkin-independent. (**B**) Differences in the percentage of TOMM20- and NDUFA4L2-positive EVs reflect the relative composition of mitochondrial vesicles and indicate distinct EV biogenesis pathways.

8.4 PDOs carrying mitophagy defects preferentially activate the Warburg effect

Given that the release of mitochondrial-derived vesicles is considered a compensatory response to mitochondrial damage when mitophagy is impaired, we aimed to determine whether differences in mitochondrial contents, reported for B250- and B211-derived secretomes, reflected distinct levels of mitochondrial dysfunction. We first evaluated the

metabolic profiles of the two PDO lines by monitoring the ATP production through Cell Titer Glow assay during six hours of treatment with oligomycin and 2-deossi-glucose, already chosen for 2D cell- experiments (**Fig. 8A**). The assay revealed that both PDOs exhibited a higher bioenergetic dependence on glycolysis. In fact, the suppression of OXPHOS pushed both B250 and B211 to deal with ATP decrease by accelerating glycolytic flux to finally restore and even overcome starting ATP levels. On the other hand, the inhibition of glycolysis did not provide the same adaptative response, leading ATP levels to gradually collapse, especially for B250 cells. These results were also consistent with ultrastructural observations, which revealed a significant number of mitochondria with enlarged and progressively disorganized cristae in both cell types. However, mega-mitochondria were observed only in B250 cells (**Fig. 8B**), suggesting more pronounced mitochondrial damage in this PDO line.

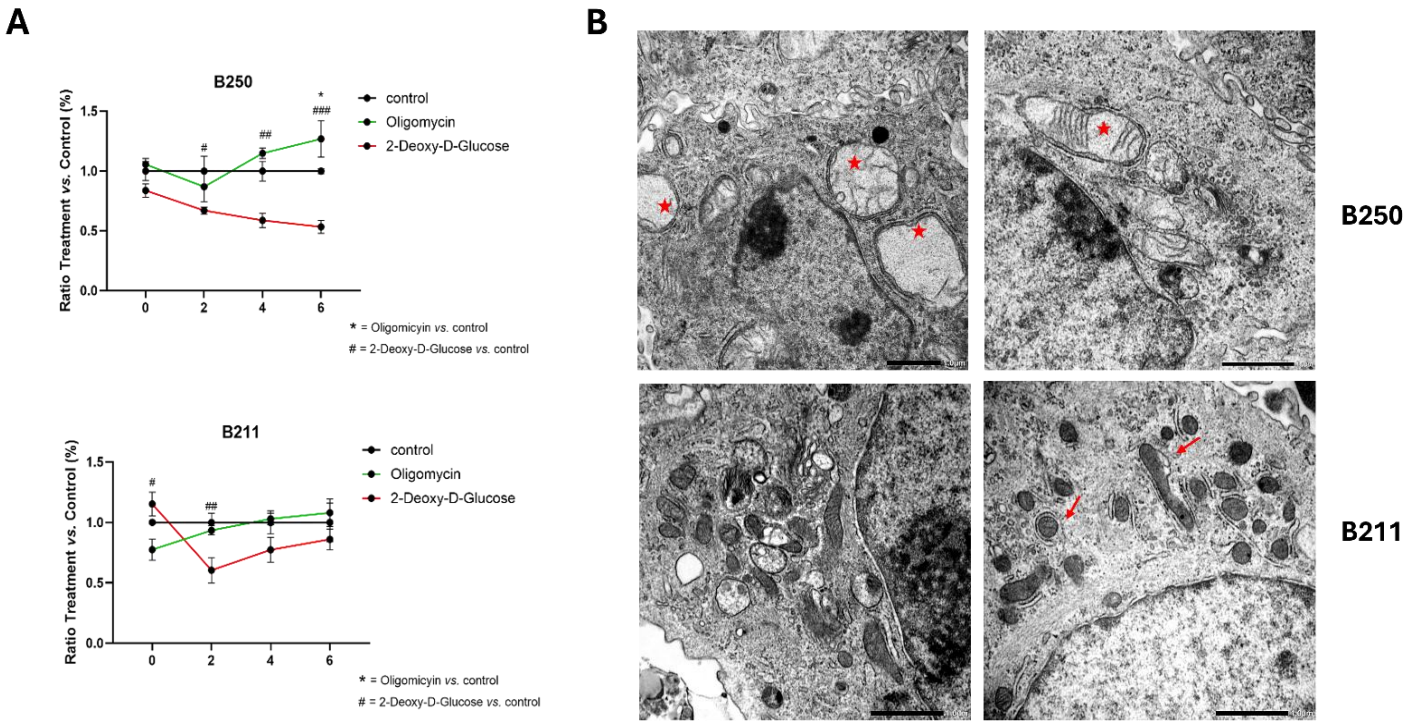


Figure 8. (**A)** In the early phase of treatment (first two hours), B250 and B211 organoids exhibit a sharp decrease in ATP production, followed by a prompt metabolic shift toward glycolytic mechanisms, consistent with the Warburg effect. Statistical analysis was performed using two-way ANOVA ($p < 0.05$). (**B**) Ultrastructural analysis reveals

mitochondrial degeneration, characterized by early-stage changes in B211 cells (red arrows) and megamitochondria in B250 cells (red stars). Magnification (8,000×; scale bar 1 μm).

8.5 *Inhibition of* $KRAS^{G12D}$ *promotes autophagy activation and modulates extracellular vesicle trafficking in glycolytic PDOs*

Cells expressing oncogenic KRAS mutations frequently exhibit impaired mitochondrial function. This condition often causes a reduced mitochondrial respiration and a consequent metabolic shift toward enhanced glycolysis (69, 102). In our study, since both B250 and B211 organoids were derived from patients with $KRAS^{G12D}$-mutated PDAC, we hypothesized that the KRAS mutation might interfere with mitochondrial function, promoting the documented metabolic reprogramming. Notably, returning to the heatmap, we noticed that organoids downregulating both mitophagy pathways share a common KRAS G12D mutant signature. This observation motivated us to explore a potential link between oncogenic KRAS and mitophagy. Thus, we aimed to assess whether the modulation of oncogenic KRAS activity might affect mitochondria turnover. For this purpose, $KRAS^{G12D}$-mutated PDOs were treated for six hours with the inhibitor MRTX-1133, which displays a high affinity for this specific oncogenic KRAS (103). From an ultrastructural perspective, treated cells showed swollen mitochondria with disrupted and reduced cristae, supporting the Warburg effect previously correlated with this category of PDOs (**Fig. 9A**). However, a pronounced increase in the number of autophagosomes, together with a greater abundance of lysosomes in close proximity, was observed in both PDO types following MRTX-1133 treatment, potentially reflecting a reactivation of the mitophagy machinery. Furthermore, in contrast to treated samples, where no evident extracellular cargos were found, untreated samples displayed frequent vesicular structures distributed in the extracellular space, often appearing as multivesicular bodies (**Fig. 9B**). Together, these observations support a potential involvement of mutant KRAS in regulating mitochondrial homeostasis through mitophagy.

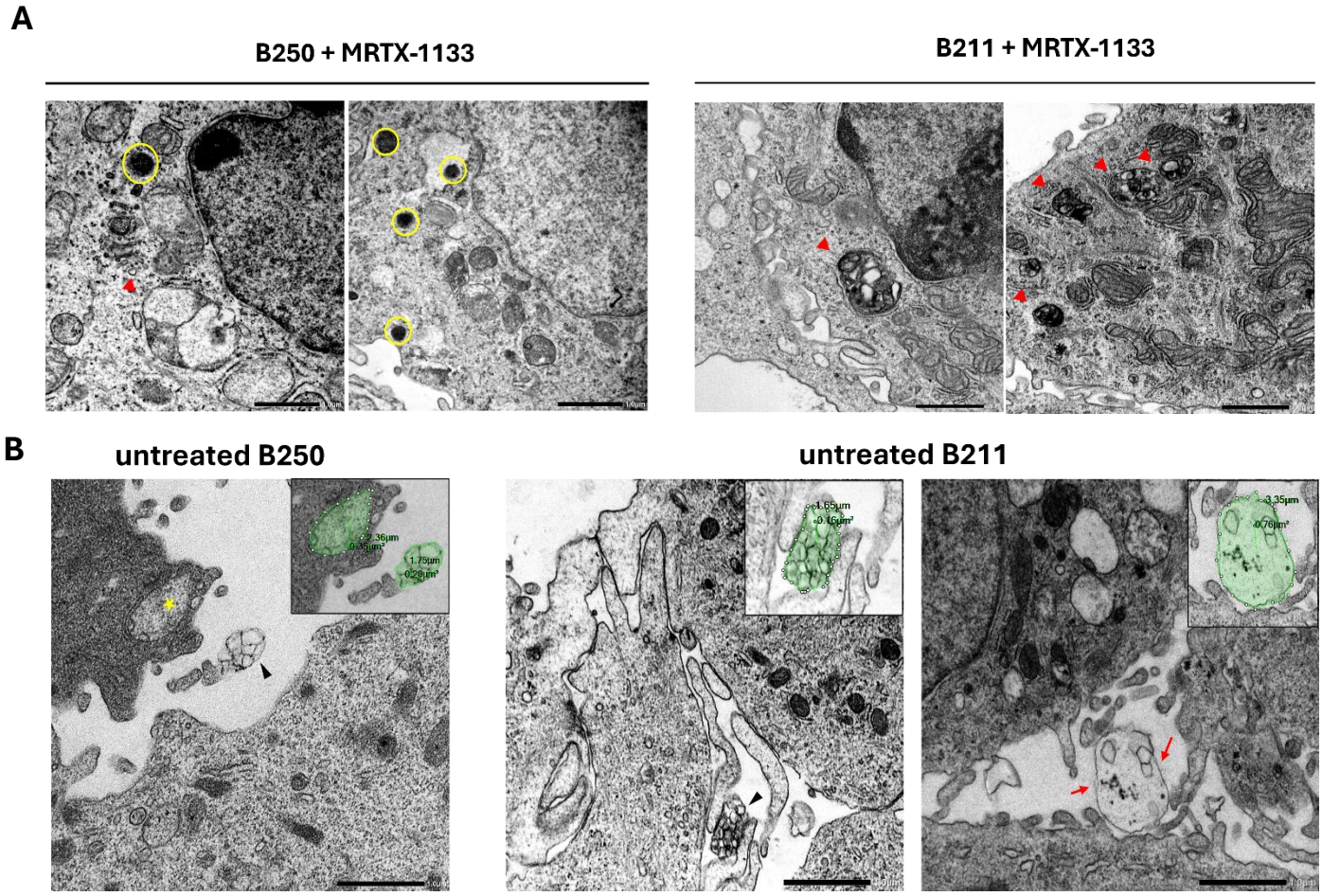


Figure 9. (**A**) An increased number of autophagosomes (red arrowheads) and lysosomes (yellow circles) closely associated with mitochondria is observed. Magnification (8,000×; scale bar 1 μm). (**B**) Evidence of multivesicular bodies in untreated samples. Insets show morphometric analyses of perimeter and area, revealing consistent sizes across the observed structures. Multivesicular bodies are captured at different stages and locations: adjacent to the plasma membrane during vesicle release (yellow star), fully formed (black arrowheads), or discharged into the extracellular space (red arrows). Magnification (8,000×; scale bar 1 μm).

Interestingly, the analysis of the derived-secretomes confirmed a divergent impact on the presence of mitochondrial components after MRTX-1133 treatment: while in B250 cells the inhibition of $KRAS^{G12D}$ correlated with a marked reduction in percentage of vesicles positive

for both TOMM20 and NDUFA4L2, a reverse effect was observed in B211 cells. This suggests that mutant KRAS might differentially interfere with the fate of damaged mitochondria (**Fig. 10**).

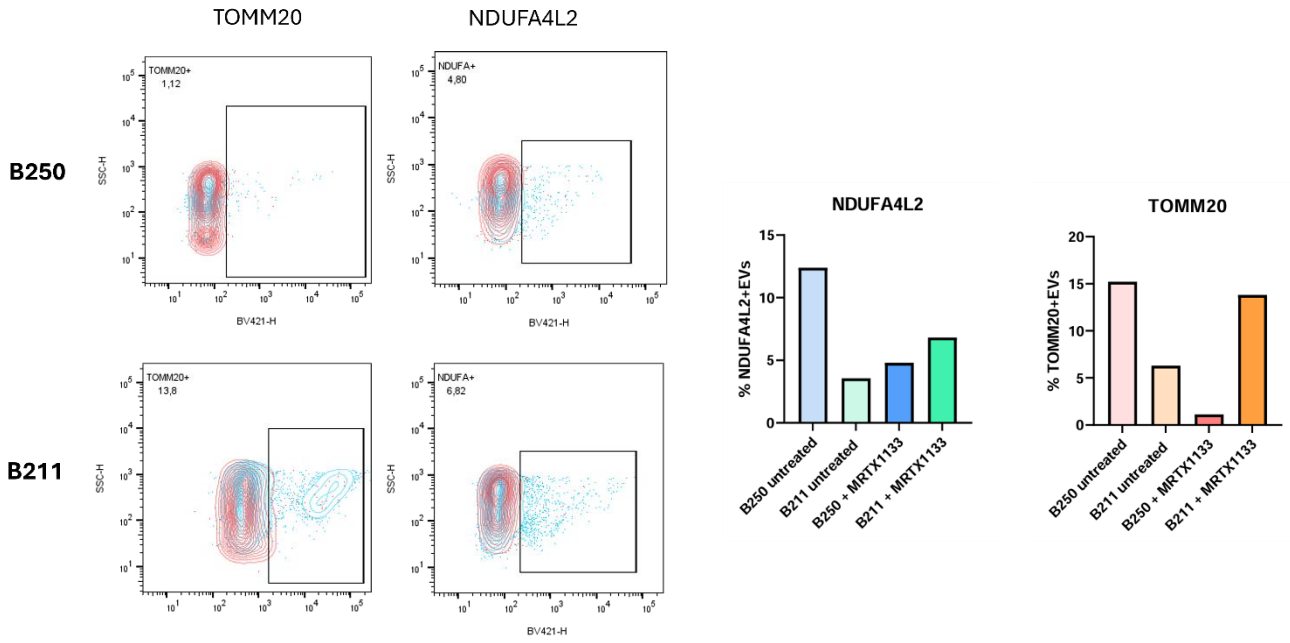


Figure 10. Comparison of NDUFA4L2 and TOMM20 content in the secretomes of untreated cells and cells treated with a KRAS inhibitor.

8.6 MRTX-1133 treatment increases PINK-1 recruitment to the OMM, supporting mitophagy induction

We subsequently investigated potential changes in the expression and localization of key mediators of the mitophagic process. As discussed above, the most well-characterized mitophagic pathway depends on Parkin activation, which is regulated by the kinase PINK-1. However, to be the real initiator of the process, PINK-1 needs to be localized on the OMM, thereby escaping constitutive proteasomal degradation. Interestingly, even in the absence of the inhibitor, PINK-1 rarely colocalized with PDH, an inner mitochondrial membrane marker, suggesting a preferential localization on the outer mitochondrial membrane. Following treatment, we observed an increased PINK-1 signal, which is consistent with our

previous ultrastructural evidence supporting the induction of mitophagy by MRTX-1133 (**Fig 11**).

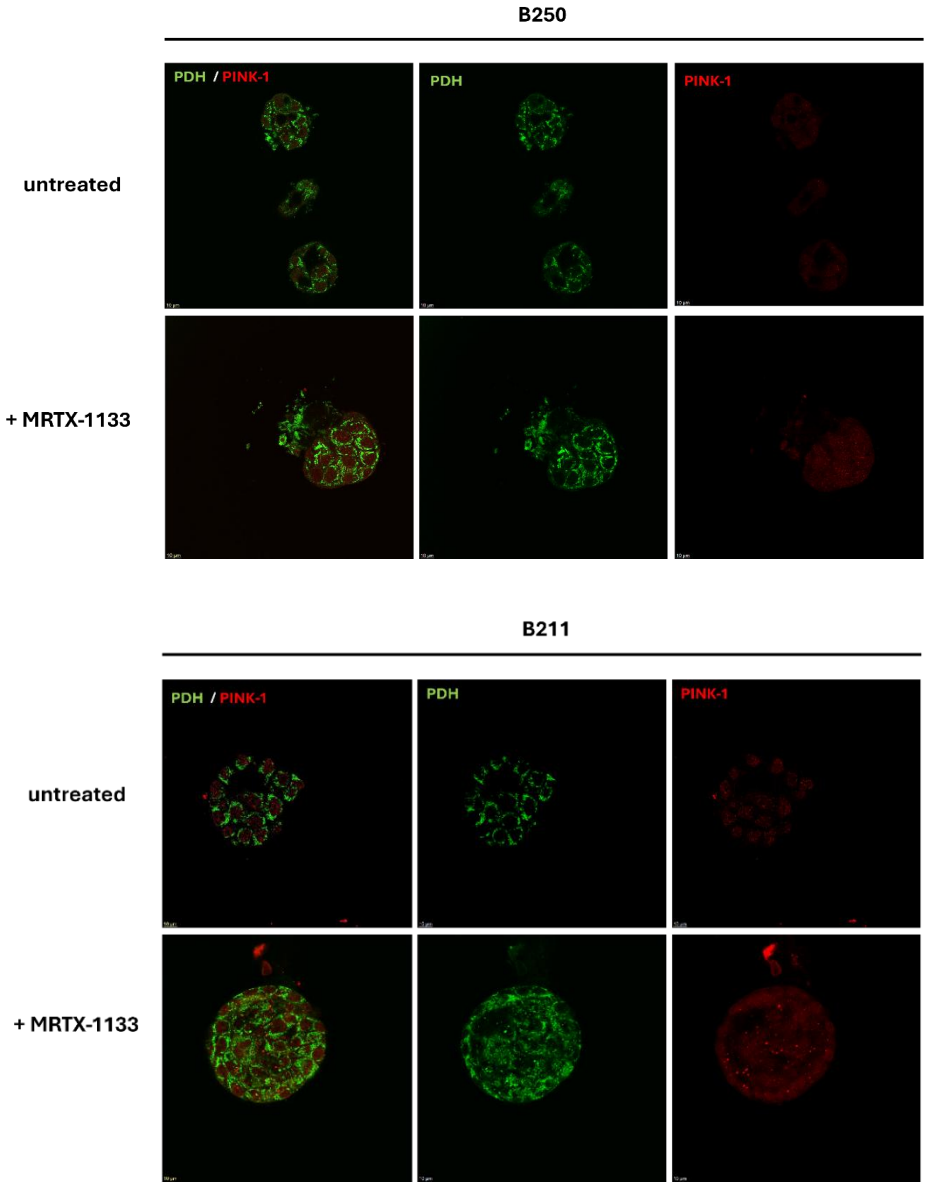


Figure 11. Immunofluorescence analysis of PINK-1 and co-localization with PDH in PDOs**.** PINK-1 predominantly localizes to the outer mitochondrial membrane (OMM), showing minimal colocalization with the inner membrane marker PDH. Upon MRTX-1133 treatment, a modest increase in PINK-1 intensity was observed, supporting the potential induction of mitophagy within these PDOs**.**

9. Discussion

The high plasticity of cancer is largely dependent on the complexity of the tumor microenvironment. A heterogenous system comprising different cell types can enhance the reciprocal signal processing capacity among cells more than a homotypic system. For this reason, pancreatic cancer (PC), developing in such a hetero-cellular environment, gradually increases its impenetrability and simultaneously becomes more aggressive. As discussed above, the high survival capability attributed to PC is also dependent on the energetic cross-talk with stromal cells, where mitochondria emerge as pivotal actors (104). Previous studies have demonstrated that mitochondrial performance can be regulated in both cancer and stromal cells via bidirectional cross-talk, often driven by oncogenes. In this regard, mutant *KRAS*^{G12D} was found to enhance metabolic networks and extend PDAC cell signaling by engaging tumor-associated fibroblasts (105). Interestingly, while it promotes a shift toward a non-respiratory phenotype in isolated PDAC cells, co-culture systems combining stroma and tumor show a restoration of mitochondrial efficiency, suggesting that oncogene-mediated effects on cancer metabolism are strongly context-dependent (105, 106).

Our initial purpose was to investigate whether metabolic reprogramming associated with mitochondrial dysfunction could exacerbate the release of mitochondrial-derived EVs and promote horizontal mitochondrial transfer. We also aimed at investigating whether it could be an additional strategy only acted by specific categories of PDAC cells bearing similar transcriptional signatures of impaired mitochondrial homeostasis. In the first part of the study, when we tested pancreatic cancer 2D models, already known for their opposing metabolic potentials, we interestingly observed that not all tumor cells respond similarly to mitochondrial degeneration. Under transmission electron microscope (TEM), KRAS-WT BXPC-3 cells appeared to cope with dysfunctional mitochondria by activating self-degradative (autophagic) mechanisms. Conversely, KRAS^{G12D} mutant PANC-1 cells accumulated disrupted mitochondria, which were rarely targeted for lysosomal clearance.

Consistently, PANC-1 cells exhibited a higher abundance of TOMM20^{pos} vesicles in their conditioned-media, as confirmed by mtDNA enrichment in isolated EVs (Fig.6). Together these preliminary data highlighted the greater potential of PDAC cell lines to release mitochondrial-derived extracellular vesicles and led us to suppose that the inefficient mitochondrial turnover might push certain PDAC cells to rely on vesicle-mediated extrusion of mitochondrial material, as an alternative clearance mechanism.

However, 2D models have several limitations: the lack of a structured microenvironment that orchestrates complex cell–cell or cell–matrix interactions have gradually driven scientists to find more comprehensive models. Thus, the development of 3D cultures named as "organoids" has bridged the gap between 2D *in vitro* and *in vivo* models. Organoids can mimic the spatial architecture and the functionalities of the tissues from which they have been originated, giving the opportunity to be used for more specific purposes, especially in the field of drug discovery and personalized medicine (107). For this reason, we were interested to assess whether patient-derived organoids had a similar behavior compared to bidimensional models. At the same time, we also expected a more complex scenario for data deriving from secretome. Gene Set Enrichment Analysis (GSEA) revealed that PDOs have different strategies to couple mitophagy and mitochondrial biogenesis, which in turn might affect their metabolic reprogramming in response to nutrient stress. Furthermore, we interestingly noticed a recurrent defect in the mitophagy machinery across specific PDOs subpopulations.

The consequences of impaired mitochondrial degradation - accumulation of dysfunctional mitochondria, increased ROS production, mtDNA mutations, and altered Ca2+ signaling - impact cells differently based on their nature. While normal cells are more prone to apoptosis, tumor cells may exploit these alterations. Indeed, impaired elimination of damaged mitochondria might act as an etiological factor in tumorigenesis, while functional mitophagy could mainly promote tumor progression. For example, loss-of-function mutations in the *PARK2* gene increase tumorigenesis in various cancers (108-112). Similarly, defective mitophagy due to *BNIP3* silencing resulted in a more aggressive PDAC

phenotype, in agreement with undetectable levels of *BNIP3* observed among 60% of pancreatic specimens from PDAC patients with reduced survival (113). For this reason, we initially compared established PDAC-derived organoids with a PanIN-derived organoid line, to assess differences in metabolic and secretory phenotypes. Our comparison between PDAC-derived organoids and PanIN-derived lines showed that PDOs with downregulated mitophagy genes exhibited a more glycolytic phenotype (Warburg effect) and a distinctive secretory pattern, characterized by increased mitochondrial content in EVs, particularly regarding the marker NDUFA4L2.

The evidence of NADH dehydrogenase [ubiquinone] 1 alpha subcomplex subunit 4–like 2 (NDUFA4L2) as cargo within the EVs, rather than TOMM20, might be indicative of a selective release of specific mitochondrial components by tumor cells. NDUFA4L2 is a mitochondrial protein that regulates oxidative phosphorylation and cellular metabolic adaptation, especially under stress conditions such as hypoxia and cancer (114). In cells displaying the Warburg effect, mitochondrial respiration is reduced, and energy production relies predominantly on glycolysis. When this metabolic state is coupled with impaired mitophagy, mitochondrial components such as NDUFA4L2 may accumulate and be redirected into EVs, potentially perturbing the extracellular space.

Our evidence suggests that, while pre-neoplastic organoids retain efficient mitochondrial quality control, multiple PDAC PDOs tend to display reduced mitophagy and a concomitant increase in the release of mito-EVs. This leads us to speculate that the exocytosis of mito-EVs, connected to dysregulated pathways of mitochondrial turnover, may not represent merely a compensatory mechanism, but could also function as a means of promoting pro-tumorigenic interactions. Consistent with our hypothesis, recent *in vitro* and *in vivo* experiments from Ikeda *et al.* (115) demonstrated that mitochondria are actively delivered from cancer cells to tumor-infiltrating lymphocytes (TILs) where they can progressively replace the local mitochondria. Interestingly, this process is enabled by the reduced susceptibility of transferred mitochondria to mitophagy in T cells, due to the presence of mitophagy-inhibitory factors such as USP30 derived from cancer cells. As a

result, mutated mitochondria persist within TILs, whereas endogenous T-cell mitochondria are preferentially eliminated through mitophagy. Indeed, defects of mitochondrial–lysosomal signaling have been reported in ovarian cancer, thereby inducing the delivery of mitochondria-derived vesicles to neighboring cells (116).

Simultaneously, a growing body of literature is now focusing on elucidating the biological consequences of mitochondrial transfer, which in most studies seems to predominantly benefit tumor progression, by increasing chemoresistance (116) or by weaking the antitumor response (115). In this perspective, the choice to mainly select altered mitochondrial components for the delivery, seems to be not so random: as Yosuke Togashi explained (117), cancer-derived dysfunctional mitochondria are more capable to "poison" the microenvironment, thereby exerting a stronger influence in disrupting and reprogramming its metabolic and signaling balance. The study by Vikramdeo and colleagues additionally proposed mutant mtDNA, identified in circulating EVs, as a potential non-invasive diagnostic marker for pancreatic cancer (118). Interestingly, they found that patients with PDAC had a higher yield of circulating EVs enriched of altered mtDNA compared with non-cancer individuals. Collectively, these findings suggest that pancreatic tumors may reprogram the internal mitochondrial homeostasis to enhance mitochondrial dysfunction and promote extracellular mitochondrial transfer, thereby supporting their progression.

Conversely, it is important to consider that the GSEA heatmap also identified a substantial subset of PDOs characterized by an upregulated mitophagy signature. Therefore, a deeper characterization of the metabolic and secretory profiles of this subset is required to further substantiate our hypothesis. Interestingly, many of these organoids display a wild-type KRAS genotype, in contrast to those with suppressed mitophagy, which are predominantly associated with recurrent KRAS mutations. Hence, the different KRAS- signatures characterizing these subpopulations pushed us to investigate any relevant effects after the targeted inhibition of $KRAS^{G12D}$. For this purpose, the small molecule inhibitor MRTX-1133 was chosen to selectively target the oncogenic protein.

Developed in 2021 (103), MRTX-1133 showed relevant antitumor efficacy both *in vitro* and *in vivo* especially against $KRAS^{G12D}$-mutant pancreatic cancer cells, where it caused the downregulation of cell cycle regulator and pro-survival genes, and the concomitant upregulation of pro-apoptotic genes (103). Therefore, based on these encouraging results, MRTX-1133 has entered a phase I/II clinical trial (119) involving patients with PDAC, colorectal cancer and other solid tumors characterized by KRAS mutations (120). However, a recent study also reported that certain types of PDAC cells are able to develop an adaptative response to MRTX-1133 treatment which involves the mechanism of autophagy. Although the drug inhibitor prevented cell growth in all four $KRAS^{G12D}$ PDAC cell lines, a marked increase in autophagic flux was detected in two of them, correlating with a lower effectiveness of MRTX-1133 treatment. These data suggested a potential resistance by those cells which can be promptly overcome by combining MRTX-1133 with chloroquine, a common autophagy inhibitor (121). Notably, when we tested the responsiveness of B250 and B211 organoids to treatment, an increase of autophagic structures was noticed under transmission electron microscope. However, these structures were frequently observed near damaged mitochondria, which were often surrounded by phagophores. This spatial association suggests that, in these conditions, MRTX-1133 may specifically interfere with mitochondrial clearance pathways. Thus, inhibition of $KRAS^{G12D}$ appeared to be associated with a restoration of mitophagic activities. However, secretome analysis did not show consistent changes in vesicle cargo, indicating that the KRAS signature may not directly influence all vesicle types. Additional functional validation studies are required to better determine whether the restoration of the mitophagy machinery in these PDAC cells is linked to more complex mechanisms rather than to an intrinsic resistance to treatment.

Notably, our investigation into the modulation of key factors involved in mitochondrial degradation and secretory activity is consistent with emerging literature. Mitophagy has been shown to limit the extracellular release of mtDNA following cellular damage; accordingly, the deletion of key mitophagy genes has been found to increase circulating mtDNA levels (122). In this context, while the leakage of mitochondrial material was previously reported to occur in the absence of Parkin expression (25), Rabas *et al.* have

recently demonstrated that PINK-1 is critical for driving the packaging of mtDNA into EVs. Interestingly, this process appears to be independent of its kinase activity (123). Collectively, these findings point to a previously unrecognized role of PINK-1 in the biogenenesis of mtDNA-containing EVs, a function mechanistically distinct from its canonical role in mitophagy. Furthermore, these insights may explain our observation that PINK-1 signal remains detectable and broadly distributed even in untreated conditions, where RNA-seq data indicated a downregulation of the entire Parkin-dependent mitophagy pathway.

In conclusion, our study supports the potential use of mitochondria-derived vesicles markers for PDAC diagnosis. We identify NDUFA4L2 as a particularly promising candidate for a more specific diagnostic approach, because of its functional relevance in tumor-driven reprogramming. In this context, the detection of NDUFA4L2 may be more indicative of an active and targeted secretory phenotype adopted by pancreatic cancer cells. Since PDAC-derived EVs were shown to promote metastasis (124) and in light of the benefits associated with horizontal mitochondrial transfer, future studies should investigate the role of NDUFA4L2-enriched EVs in altering the stromal cell phenotype. Additionally, clarifying whether this selective delivery correlates with tumor aggressiveness could improve patient stratification and support the development of more personalized therapeutic strategies, including the selection of the most appropriate chemotherapeutic agent.

References

1. Siegel RL, Miller KD, Wagle NS, Jemal A. Cancer statistics, **2023**. CA Cancer J Clin. 2023 Jan;73(1):17-48. doi: 10.3322/caac.21763.
2. Giansante V, Stati G, Sancilio S, Guerra E, Alberti S, Di Pietro R. The Dual Role of Necroptosis in Pancreatic Ductal Adenocarcinoma. Int J Mol Sci. **2023** Aug 10;24(16):12633. doi: 10.3390/ijms241612633.

3. Bosetti C, Lucenteforte E, Silverman DT et al. Cigarette smoking and pancreatic cancer: an analysis from the International Pancreatic Cancer Case-Control Consortium (Panc4). Ann Oncol. 2012; 23(7):1880–1888. doi: 10.1093/annonc/mdr541
4. Wang YT, Gou YW, Jin WW, Xiao M, Fang HY. Association between alcohol intake and the risk of pancreatic cancer: a dose-response meta-analysis of cohort studies. BMC Cancer. **2016**;16:212. doi: 10.1186/s12885-016-2241-
5. Raimondi S, Lowenfels AB, Morselli-Labate AM, Maisonneuve P, Pezzilli R. Pancreatic cancer in chronic pancreatitis; aetiology, incidence, and early detection. Best Pract Res Clin Gastroenterol. **2010**;24:349–358. doi: 10.1016/j.bpg.2010.02.007.
6. Larsson SC, Orsini N, Wolk A. Body mass index and pancreatic cancer risk: A meta-analysis of prospective studies. Int J Cancer. **2007**;120:1993–1998. doi: 10.1002/ijc.22535.
7. Haeberle L, Esposito I. Pathology of pancreatic cancer. Transl Gastroenterol Hepatol. **2019** Jun 27;4:50. doi: 10.21037/tgh.2019.06.02
8. Park W, Chawla A, O'Reilly EM. Pancreatic Cancer: A Review. JAMA. **2021** Sep 7;326(9):851-862. doi: 10.1001/jama.2021.13027. Erratum in: JAMA. 2021 Nov 23;326(20):2081. doi: 10.1001/jama.2021
9. Hu C, Hart SN, Polley EC, et al. Association between inherited germline mutations in cancer predisposition genes and risk of pancreatic cancer. JAMA. **2018**;319(23):2401–2409. doi: 10.1001/jama.2018.6228
10. Moffitt RA, Marayati R, Flate EL, Volmar KE, Loeza SG, Hoadley KA, Rashid NU, Williams LA, Eaton SC, Chung AH et al. Virtual microdissection identifies distinct tumor- and stroma-specific subtypes of pancreatic ductal adenocarcinoma. Nat. Genet. **2015**;47:1168–1178. doi: 10.1038/ng.3398
11. Norton J, Foster D, Chinta M, Titan A, Longaker M. Pancreatic Cancer Associated Fibroblasts (CAF): Under-Explored Target for Pancreatic Cancer Treatment. Cancers. **2020**;12:1347. doi: 10.3390/cancers12051347.
12. Kleeff J, Korc M, Apte M, La Vecchia C, Johnson CD, Biankin AV, Neale RE, Tempero M, Tuveson DA, Hruban RH et al. Pancreatic cancer. Nat. Rev. Dis. Primers. **2016**;2:16022. doi: 10.1038/nrdp.2016.22

13. Zhang A, Qian Y, Ye Z, Chen H, Xie H, Zhou L, Shen Y, Zheng S. Cancer-associated fibroblasts promote M2 polarization of macrophages in pancreatic ductal adenocarcinoma. Cancer Med. **2017**;6:463–470. doi: 10.1002/cam4.993
14. Wu Y, Zhang C, Jiang K, Werner J, Bazhin AV, D'Haese JG. The Role of Stellate Cells in Pancreatic Ductal Adenocarcinoma: Targeting Perspectives. Front. Oncol. **2021**;10:621937. doi: 10.3389/fonc.2020.621937
15. Chen ZG, Wang Y, Fong WP, Hu MT, Liang JY, Wang L, Li YH. A quantitative score of immune cell infiltration predicts the prognosis in pancreatic ductal adenocarcinoma. Int. Immunopharmacol. **2021**;98:107890. doi: 10.1016/j.intimp.2021.107890
16. Mercanti L, Sindaco M, Mazzone M, Di Marcantonio MC, Piscione M, Muraro R, Mincione G. PDAC, the Influencer Cancer: Cross-Talk with Tumor Microenvironment and Connected Potential Therapy Strategies. Cancers (Basel). **2023** May 26;15(11):2923. doi: 10.3390/cancers15112923
17. Das S, Shapiro B, Vucic EA, Vogt S, Bar-Sagi D. Tumor Cell-Derived IL1β Promotes Desmoplasia and Immune Suppression in Pancreatic Cancer. Cancer Res. **2020**;80:1088–1101. doi: 10.1158/0008-5472.CAN-19-2080
18. Roca-Portoles A, Tait SWG. Mitochondrial quality control: from molecule to organelle. Cell Mol Life Sci. **2021**;78(8):3853–66. doi: 10.1007/s00018-021-03775-0.
19. Tang C, Cai J, Yin XM, Weinberg JM, Venkatachalam MA, Dong Z. Mitochondrial quality control in kidney injury and repair. Nat Rev Nephrol. **2021** May;17(5):299-318. doi: 10.1038/s41581-020-00369-0.
20. Liu, BH., Xu, CZ., Liu, Y. *et al*. Mitochondrial quality control in human health and disease. *Military Med Res* **2024**; 11, 32. doi:10.1186/s40779-024-00536-5
21. Onishi M, Yamano K, Sato M, Matsuda N, Okamoto K. Molecular mechanisms and physiological functions of mitophagy. EMBO J. **2021** Feb 1;40(3):e104705. doi: 10.15252/embj.2020104705
22. Gustafsson AB, Dorn GW. 2nd Evolving and expanding the roles of mitophagy as a homeostatic and pathogenic process Physiol. Rev., **2019**; 99 (1) pp. 853-892

23. Chan NC, Salazar AM, Pham AH, Sweredoski MJ, Kolawa NJ, Graham RL, Hess S, Chan DC. Broad activation of the ubiquitin-proteasome system by Parkin is critical for mitophagy. Hum Mol Genet. **2011** May 1;20(9):1726-37. doi: 10.1093/hmg/ddr048.
24. Zhang J, Ney PA. Role of BNIP3 and NIX in cell death, autophagy, and mitophagy. Cell Death Differ. **2009** Jul;16(7):939-46. doi: 10.1038/cdd.2009.16.
25. Todkar, K, Chikhi L, Desjardins V, El-Mortada F, Pépin G, Germain M. rabPackaging of Mitochondrial proteins into extracellular vesicles prevents the release of mitochondrial DAMPs. *Nat. Commun.* **2021**, *12*, 1971. doi: 10.1038/s41467-021-21984-w.
26. Picca A, Guerra F, Calvani R, Coelho-Júnior HJ. Landi F, Bucci C, Marzetti E. Mitochondrial-Derived Vesicles: The Good, the Bad, and the Ugly. *Int. J. Mol. Sci.* **2023**, *24*, 13835. doi: 10.3390/ijms241813835
27. Ferrucci L, Guerra F, Bucci C, Marzetti E, Picca A. Mitochondria break free: Mitochondria-derived vesicles in aging and associated conditions. Ageing Res Rev. **2024** Dec;102:102549. doi: 10.1016/j.arr.2024.102549.
28. Neuspiel M, Schauss AC, Braschi E, Zunino R, Rippstein P, Rachubinski RA, Andrade-Navarro MA, McBride HM. Cargo-selected transport from the mitochondria to peroxisomes is mediated by vesicular carriers. Curr Biol. **2008** Jan 22;18(2):102-8. doi: 10.1016/j.cub.2007.12.038.
29. McLelland GL, Soubannier V, Chen CX, McBride HM, Fon EA. Parkin and PINK1 function in a vesicular trafficking pathway regulating mitochondrial quality control. EMBO J. **2014** Feb 18;33(4):282-95. doi: 10.1002/embj.201385902.
30. Heyn J, Heuschkel MA, Goettsch C. Mitochondrial-Derived Vesicles—Link to Extracellular Vesicles and Implications in Cardiovascular Disease. *Int. J. Mol. Sci.* **2023**, *24*, 2637. https://doi.org/10.3390/ijms24032637
31. Vasam G, Nadeau R, Cadete VJJ, Lavallée-Adam M, Menzies KJ, Burelle Y. Proteomics characterization of mitochondrial-derived vesicles under oxidative stress. FASEB J. **2021** Apr;35(4):e21278. doi: 10.1096/fj.202002151R.

32. Soubannier V, Rippstein P, Kaufman BA, Shoubridge EA, McBride HM. Reconstitution of mitochondria derived vesicle formation demonstrates selective enrichment of oxidized cargo. PLoS One. **2012**;7(12):e52830. doi: 10.1371/journal.pone.0052830.
33. Dixson AC, Dawson TR, Di Vizio D, Weaver AM. Context-specific regulation of extracellular vesicle biogenesis and cargo selection. Nat Rev Mol Cell Biol. **2023** Jul;24(7):454-476. doi: 10.1038/s41580-023-00576-0.
34. Zhou X, Liu S, Lu Y, Wan M, Cheng J, Liu J. MitoEVs: A new player in multiple disease pathology and treatment. J Extracell Vesicles. **2023** Apr;12(4):e12320. doi: 10.1002/jev2.12320
35. Crewe C, Funcke JB, Li S, Joffin N, Gliniak CM, Ghaben AL, An YA, Sadek HA, Gordillo R, Akgul Y, Chen S, Samovski D, Fischer-Posovszky P, Kusminski CM, Klein S, Scherer PE. Extracellular vesicle-based interorgan transport of mitochondria from energetically stressed adipocytes. Cell Metab. **2021** Sep 7;33(9):1853-1868.e11. doi: 10.1016/j.cmet.2021.08.002
36. Ikeda G, Santoso MR, Tada Y, Li AM, Vaskova E, Jung JH, O'Brien C, Egan E, Ye J, Yang PC. Mitochondria-Rich Extracellular Vesicles From Autologous Stem Cell-Derived Cardiomyocytes Restore Energetics of Ischemic Myocardium. J Am Coll Cardiol. **2021** Mar 2;77(8):1073-1088. doi: 10.1016/j.jacc.2020.12.060
37. Rosina M, Ceci V, Turchi R, Chuan L, Borcherding N, Sciarretta F, Sánchez-Díaz M, Tortolici F, Karlinsey K, Chiurchiù V, Fuoco C, Giwa R, Field RL, Audano M, Arena S, Palma A, Riccio F, Shamsi F, Renzone G, Verri M, Crescenzi A, Rizza S, Faienza F, Filomeni G, Kooijman S, Rufini S, de Vries AAF, Scaloni A, Mitro N, Tseng YH, Hidalgo A, Zhou B, Brestoff JR, Aquilano K, Lettieri-Barbato D. Ejection of damaged mitochondria and their removal by macrophages ensure efficient thermogenesis in brown adipose tissue. Cell Metab. **2022** Apr 5;34(4):533-548.e12. doi: 10.1016/j.cmet.2022.02.016
38. Awad AMAM, Abdul Karim N. Dysregulation of Mitochondrial Function in Cancer Cells. *Int. J. Mol. Sci.* **2025**, *26*, 6750. doi: 10.3390/ijms26146750

39. Desousa BR, Kim KK, Jones AE, Ball AB, Hsieh WY, Swain P, Morrow DH, Brownstein AJ, Ferrick DA, Shirihai OS, Neilson A, Nathanson DA, Rogers GW, Dranka BP, Murphy AN, Affourtit C, Bensinger SJ, Stiles L, Romero N, Divakaruni AS. Calculation of ATP production rates using the Seahorse XF Analyzer. EMBO Rep. **2023** Oct 9;24(10):e56380. doi: 10.15252/embr.202256380.
40. Srinivasan S, Guha M, Kashina A, Avadhani NG. Mitochondrial dysfunction and mitochondrial dynamics-The cancer connection. Biochim Biophys Acta Bioenerg. **2017** Aug;1858(8):602-614. doi: 10.1016/j.bbabio.2017.01.004.
41. Luo Y, Ma J, Lu W. The Significance of Mitochondrial Dysfunction in Cancer. Int J Mol Sci. **2020** Aug 5;21(16):5598. doi: 10.3390/ijms21165598.
42. Pelicano H., Carney D., Huang P. ROS stress in cancer cells and therapeutic implications. Drug Resist. Updates. **2004**;7:97–110. doi: 10.1016/j.drup.2004.01.004.
43. Giedt RJ, Fumene Feruglio P, Pathania D, Yang KS, Kilcoyne A, Vinegoni C, Mitchison TJ, Weissleder R. Computational imaging reveals mitochondrial morphology as a biomarker of cancer phenotype and drug response. Sci Rep. **2016** Sep 9;6:32985. doi: 10.1038/srep32985.
44. Halestrap AP. The regulation of the matrix volume of mammalian mitochondria in vivo and in vitro and its role in the control of mitochondrial metabolism. *Biochim Biophys Acta (BBA) Bioenergetics*s. **1989**; 973(3):355–82. doi: 10.1016/S0005-2728(89)80378-0
45. Bernardi P, Di Lisa F. The mitochondrial permeability transition pore: molecular nature and role as a target in cardioprotection. *J Mol Cell Cardiol* (2015) 78:100–6. doi: 10.1016/j.yjmcc.2014.09.023
46. Grieco JP, Allen ME, Perry JB, Wang Y, Song Y, Rohani A, Compton SLE, Smyth JW, Swami NS, Brown DA, Schmelz EM. Progression-Mediated Changes in Mitochondrial Morphology Promotes Adaptation to Hypoxic Peritoneal Conditions in Serous Ovarian Cancer. Front Oncol. **2021** Jan 13;10:600113. doi: 10.3389/fonc.2020.600113.
47. Hsu CC, Tseng LM, Lee HC. Role of mitochondrial dysfunction in cancer progression. Exp. Biol. Med. **2016**;241:1281–1295. doi: 10.1177/1535370216641787

48. Yin PH, Wu CC, Lin JC, Chi CW, Wei YH, Lee HC. Somatic mutations of mitochondrial genome in hepatocellular carcinoma. Mitochondrion. **2010**;10:174–182. doi: 10.1016/j.mito.2009.12.147.
49. Tseng LM, Yin PH, Yang CW, Tsai YF, Hsu CY, Chi CW, Lee HC. Somatic mutations of the mitochondrial genome in human breast cancers. Genes Chromosom. Cancer. **2011**;50:800–811. doi: 10.1002/gcc.20901
50. Lee HC, Huang KH, Yeh TS, Chi CW. Somatic alterations in mitochondrial DNA and mitochondrial dysfunction in gastric cancer progression. World J. Gastroenterol. **2014**;20:3950–3959. doi: 10.3748/wjg.v20.i14.3950
51. Larman TC, DePalma SR, Hadjipanayis AG, Protopopov A, Zhang J, Gabriel SB, Chin L, Seidman CE, Kucherlapati R, Cancer Genome Atlas Research Network Spectrum of somatic mitochondrial mutations in five cancers. Proc. Natl. Acad. Sci. USA. **2012**;109:14087–14091. doi: 10.1073/pnas.1211502109
52. Sarwar A, Zhu M, Su Q, Zhu Z, Yang T, Chen Y, Peng X, Zhang Y. Targeting mitochondrial dysfunctions in pancreatic cancer evokes new therapeutic opportunities. Crit Rev Oncol Hematol. **2022** Dec;180:103858. doi: 10.1016/j.critrevonc.2022.103858..
53. Hardie RA, van Dam E, Cowley M, Han TL, Balaban S, Pajic M, Pinese M, Iconomou M, Shearer RF, McKenna J, Miller D, Waddell N, Pearson JV, Grimmond SM; Australian Pancreatic Cancer Genome Initiative; Sazanov L, Biankin AV, Villas-Boas S, Hoy AJ, Turner N, Saunders DN. Mitochondrial mutations and metabolic adaptation in pancreatic cancer. Cancer Metab. **2017** Jan 30;5:2. doi: 10.1186/s40170-017-0164-1.
54. Tuchalska-Czuroń J, Lenart J, Augustyniak J, Durlik M. Is mitochondrial DNA copy number a good prognostic marker in resectable pancreatic cancer? Pancreatology. **2019** Jan;19(1):73-79. doi: 10.1016/j.pan.2018.11.009.
55. Zhao J, Zhang J, Yu M, Xie Y, Huang Y, Wolff DW, Abel PW, Tu Y. Mitochondrial dynamics regulates migration and invasion of breast cancer cells. Oncogene. **2013** Oct;32(40):4814-24. doi: 10.1038/onc.2012.494.

56. Chen X, Yang P, Qiao Y, Ye F, Wang Z, Xu M, Han X, Song L, Wu Y, Ou WB. Effects of cancer-associated point mutations on the structure, function, and stability of isocitrate dehydrogenase 2. Sci Rep. **2022** Nov 5;12(1):18830. doi: 10.1038/s41598-022-23659-y.
57. Anderson GR, Wardell SE, Cakir M, Yip C, Ahn YR, Ali M, Yllanes AP, Chao CA, McDonnell DP, Wood KC. Dysregulation of mitochondrial dynamics proteins are a targetable feature of human tumors. Nat Commun. **2018** Apr 26;9(1):1677. doi: 10.1038/s41467-018-04033-x
58. Towers CG, Wodetzki DK, Thorburn J, Smith KR, Caino MC, Thorburn A. Mitochondrial-derived vesicles compensate for loss of LC3-mediated mitophagy. Dev Cell. **2021** Jul 26;56(14):2029-2042.e5. doi: 10.1016/j.devcel.2021.06.003
59. Sarwar A, Zhu M, Su Q, Zhu Z, Yang T, Chen Y, Peng X, Zhang Y. Targeting mitochondrial dysfunctions in pancreatic cancer evokes new therapeutic opportunities. Crit Rev Oncol Hematol. **2022** Dec;180:103858. doi: 10.1016/j.critrevonc.2022
60. Reyes-Castellanos G, Masoud R, Carrier A. Mitochondrial Metabolism in PDAC: From Better Knowledge to New Targeting Strategies. Biomedicines. **2020** Aug 3;8(8):270. doi: 10.3390/biomedicines8080270.
61. Daemen A, Peterson D, Sahu N, McCord R, Du X, Liu B, Kowanetz K, Hong R, Moffat J, Gao M, Boudreau A, Mroue R, Corson L, O'Brien T, Qing J, Sampath D, Merchant M, Yauch R, Manning G, Settleman J, Hatzivassiliou G, Evangelista M. Metabolite profiling stratifies pancreatic ductal adenocarcinomas into subtypes with distinct sensitivities to metabolic inhibitors. Proc Natl Acad Sci U S A. **2015** Aug 11;112(32):E4410-7. doi: 10.1073/pnas.1501605112
62. Hensley CT, Wasti AT, DeBerardinis RJ. Glutamine and cancer: cell biology, physiology, and clinical opportunities. J Clin Invest. **2013** Sep;123(9):3678-84. doi: 10.1172/JCI69600.
63. Achreja A, Zhao H, Yang L, Yun TH, Marini J, Nagrath D. Exo-MFA - A 13C metabolic flux analysis framework to dissect tumor microenvironment-secreted exosome contributions towards cancer cell metabolism. Metab Eng**. 2017** Sep;43(Pt B):156-172. doi: 10.1016/j.ymben.2017.01.001.

64. Olivares O, Mayers J, Gouirand V. *et al.* Collagen-derived proline promotes pancreatic ductal adenocarcinoma cell survival under nutrient limited conditions. *Nat Commun.* **2017;** 8, 16031. doi: 10.1038/ncomms16031

65. Chan-Seng-Yue M, Kim JC, Wilson GW, Ng K, Figueroa EF, O'Kane GM, Connor AA, Denroche RE, Grant RC, McLeod J, Wilson JM, Jang GH, Zhang A, Dodd A, Liang SB, Borgida A, Chadwick D, Kalimuthu S, Lungu I, Bartlett JMS, Krzyzanowski PM, Sandhu V, Tiriac H, Froeling FEM, Karasinska JM, Topham JT, Renouf DJ, Schaeffer DF, Jones SJM, Marra MA, Laskin J, Chetty R, Stein LD, Zogopoulos G, Haibe-Kains B, Campbell PJ, Tuveson DA, Knox JJ, Fischer SE, Gallinger S, Notta F. Transcription phenotypes of pancreatic cancer are driven by genomic events during tumor evolution. Nat Genet. **2020** Feb;52(2):231-240. doi: 10.1038/s41588-019-0566-9. Epub 2020 Jan 13. Erratum in: Nat Genet. 2020 Apr;52(4):463. doi: 10.1038/s41588-020-0588-3.

66. Yakubovskaya MS, Spiegelman V, Luo FC, Malaev S, Salnev A, Zborovskaya I, Gasparyan A, Polotsky B, Machaladze Z, Trachtenberg AC, et al. High frequency of K-ras mutations in normal appearing lung tissues and sputum of patients with lung cancer. Int J Cancer. **1995** Dec 11;63(6):810-4. doi: 10.1002/ijc.2910630611

67. Gaglio D, Metallo CM, Gameiro PA, Hiller K, Danna LS, Balestrieri C, Alberghina L, Stephanopoulos G, Chiaradonna F. Oncogenic K-Ras decouples glucose and glutamine metabolism to support cancer cell growth. Mol. Syst. Biol. **2011**;7:523. doi: 10.1038/msb.2011.56

68. Suzuki T, Otsuka M, Seimiya T, Iwata T, Kishikawa T, Koike K. The biological role of metabolic reprogramming in pancreatic cancer. MedComm. **2020** Nov 5;1(3):302-310. doi: 10.1002/mco2.37.

69. Hu Y, Lu W, Chen G, Wang P, Chen Z, Zhou Y, Ogasawara M, Trachootham D, Feng L, Pelicano H, Chiao PJ, Keating MJ, Garcia-Manero G, Huang P. K-ras(G12V) transformation leads to mitochondrial dysfunction and a metabolic switch from oxidative phosphorylation to glycolysis. Cell Res. **2012** Feb;22(2):399-412. doi: 10.1038/cr.2011.145

70. Liu D, Gao Y, Liu J, Huang Y, Yin J, Feng Y, Shi L, Meloni BP, Zhang C, Zheng M, Gao J. Intercellular mitochondrial transfer as a means of tissue revitalization. Signal Transduct Target Ther. **2021** Feb 16;6(1):65. doi: 10.1038/s41392-020-00440-z.
71. Torralba D, Baixauli F, Sánchez-Madrid F. Mitochondria Know No Boundaries: Mechanisms and Functions of Intercellular Mitochondrial Transfer. Front Cell Dev Biol. **2016** Sep 28;4:107. doi: 10.3389/fcell.2016.00107.
72. Uspenskaya, Y.A., Malinovskaya, N.A. & Salmina, A.B. Intercellular Transport of Mitochondria: Molecular Mechanisms and Role in Maintaining Energy Homeostasis in Tissues. *Cell Tiss. Biol.* **2022**; 16, 97–113. Doi: 10.1134/S1990519X22020109
73. Davis CH, Kim KY, Bushong EA, Mills EA, Boassa D, Shih T, Kinebuchi M, Phan S, Zhou Y, Bihlmeyer NA, Nguyen JV, Jin Y, Ellisman MH, Marsh-Armstrong N. Transcellular degradation of axonal mitochondria. Proc Natl Acad Sci U S A. **2014** Jul 1;111(26):9633-8. doi: 10.1073/pnas.1404651111.
74. Valdebenito S, Malik S, Luu R, Loudig O, Mitchell M, Okafo G, Bhat K, Prideaux B, Eugenin EA. Tunneling nanotubes, TNT, communicate glioblastoma with surrounding non-tumor astrocytes to adapt them to hypoxic and metabolic tumor conditions. Sci Rep. **2021** Jul 15;11(1):14556. doi: 10.1038/s41598-021-93775-8.
75. Solimando, A.G., Di Palma, F., Desantis, V. *et al.* Tunneling nanotubes between bone marrow stromal cells support transmitophagy and resistance to apoptosis in myeloma. *Blood Cancer J.* **2025**; 15, 3. doi: 10.1038/s41408-025-01210-2
76. Watson DC, Bayik D, Storevik S, Moreino SS, Sprowls SA, Han J, Augustsson MT, Lauko A, Sravya P, Røsland GV, Troike K, Tronstad KJ, Wang S, Sarnow K, Kay K, Lunavat TR, Silver DJ, Dayal S, Joseph JV, Mulkearns-Hubert E, Ystaas LAR, Deshpande G, Guyon J, Zhou Y, Magaut CR, Seder J, Neises L, Williford SE, Meiser J, Scott AJ, Sajjakulnukit P, Mears JA, Bjerkvig R, Chakraborty A, Daubon T, Cheng F, Lyssiotis CA, Wahl DR, Hjelmeland AB, Hossain JA, Miletic H, Lathia JD. GAP43-dependent mitochondria transfer from astrocytes enhances glioblastoma tumorigenicity. Nat Cancer. **2023** May;4(5):648-664. doi: 10.1038/s43018-023-00556-5

77. Zhang W, Zhou H, Li H, Mou H, Yinwang E, Xue Y, Wang S, Zhang Y, Wang Z, Chen T, Sun H, Wang F, Zhang J, Chai X, Chen S, Li B, Zhang C, Gao J, Ye Z. Cancer cells reprogram to metastatic state through the acquisition of platelet mitochondria. Cell Rep. **2023** Sep 26;42(9):113147. doi: 10.1016/j.celrep.2023.113147.
78. Yang Q, Cui M, Wang J, *et al.* Circulating mitochondrial DNA promotes M2 polarization of tumor associated macrophages and HCC resistance to sorafenib. *Cell Death Dis.* **2025**. 16, 153. doi: 10.1038/s41419-025-07473-8
79. Zhang G, Wei, H, Zhao A, *et al.* Mitochondrial DNA leakage: underlying mechanisms and therapeutic implications in neurological disorders. *J Neuroinflammation* **2025**, 22.34. doi: 10.1186/s12974-025-03363-0
80. Zhao Y, Wu C, Liang X, Yang M. Cell-free mitochondrial DNA as a pro-inflammatory agent in blood circulation: mechanisms, therapeutic implications, and clinical challenges in immune dysregulation. Front Immunol. **2025** Oct 1;16:1640748. doi: 10.3389/fimmu.2025.1640748.
81. Peng F, Wang S, Feng Z, Zhou K, Zhang H, Guo X, Xing J, Liu Y. Circulating cell-free mtDNA as a new biomarker for cancer detection and management. Cancer Biol Med. 2023 Oct 12;21(2):105–10. doi: 10.20892/j.issn.2095-3941.2023.0280.
82. Cubilla AL, Fitzgerald PJ. Cancer (non-endocrine) of the pancreas. A suggested classification. Monogr Pathol. **1980**;21:82-110.
83. Tannous T, Perez Rodriguez AL, Mak AW, Tannous K, Keating M. Primary Clear Cell Carcinoma of the Pancreas: A Systematic Review. Cureus. **2021** Jun 15;13(6):e15668. doi: 10.7759/cureus.15668.
84. Giansante V, Di Angelo L, Calabrese C, De Sanctis P, Regi P, Martelli FM, Stati G, Lattanzio R, Alberti S, Guerra E, Di Pietro R. Novel Ultrastructural Insights into the Clear-Cell Carcinoma of the Pancreas: A Case Report. Int J Mol Sci. **2024** Apr 13;25(8):4313. doi: 10.3390/ijms25084313.
85. Servage KA, Stefanius K, Gray HF, Orth K. Proteomic Profiling of Small Extracellular Vesicles Secreted by Human Pancreatic Cancer Cells Implicated in Cellular Transformation. Sci Rep. **2020** May 7;10(1):7713. doi: 10.1038/s41598-020-64718-6.

86. Pfleger J. Measurements of Mitochondrial Respiration in Intact Cells, Permeabilized Cells, and Isolated Tissue Mitochondria Using the Seahorse XF Analyzer. Methods Mol Biol. **2022**;2497:185-206. doi: 10.1007/978-1-0716-2309-1_12.
87. Dantes Z, Yen HY, Pfarr N, Winter C, Steiger K, Muckenhuber A, Hennig A, Lange S, Engleitner T, Öllinger R, Maresch R, Orben F, Heid I, Kaissis G, Shi K, Topping G, Stögbauer F, Wirth M, Peschke K, Papargyriou A, Rezaee-Oghazi M, Feldmann K, Schäfer AP, Ranjan R, Lubeseder-Martellato C, Stange DE, Welsch T, Martignoni M, Ceyhan GO, Friess H, Herner A, Liotta L, Treiber M, von Figura G, Abdelhafez M, Klare P, Schlag C, Algül H, Siveke J, Braren R, Weirich G, Weichert W, Saur D, Rad R, Schmid RM, Schneider G, Reichert M. Implementing cell-free DNA of pancreatic cancer patient-derived organoids for personalized oncology. JCI Insight. **2020** Aug 6;5(15):e137809. doi: 10.1172/jci.insight.
88. Hao W, Chang CP, Tsao CC, Xu J. Oligomycin-induced bioenergetic adaptation in cancer cells with heterogeneous bioenergetic organization. J Biol Chem. **2010** Apr 23;285(17):12647-54. doi: 10.1074/jbc.M109.084194.
89. Théry C, Amigorena S, Raposo G, Clayton A. Isolation and characterization of exosomes from cell culture supernatants and biological fluids. Curr Protoc Cell Biol. **2006** Apr;Chapter 3:Unit 3.22. doi: 10.1002/0471143030.cb0322s30.
90. Raposo G, Nijman HW, Stoorvogel W, Liejendekker R, Harding CV, Melief CJ, Geuze HJ. B lymphocytes secrete antigen-presenting vesicles. J Exp Med. **1996** Mar 1;183(3):1161-72. doi: 10.1084/jem.183.3.1161..
91. Tataranni T, Agriesti F, Ruggieri V, Mazzoccoli C, Simeon V, Laurenzana I, Scrima R, Pazienza V, Capitanio N, Piccoli C. Rewiring carbohydrate catabolism differentially affects survival of pancreatic cancer cell lines with diverse metabolic profiles. Oncotarget. **2017** Jun 20;8(25):41265-41281. doi: 10.18632/oncotarget.17172.
92. Marchisio M, Simeone P, Bologna G, Ercolino E, Pierdomenico L, Pieragostino D, Ventrella A, Antonini F, Del Zotto G, Vergara D, Celia C, Di Marzio L, Del Boccio P, Fontana A, Bosco D, Miscia S, Lanuti P. Flow Cytometry Analysis of Circulating

Extracellular Vesicle Subtypes from Fresh Peripheral Blood Samples. Int J Mol Sci. **2020** Dec 23;22(1):48. doi: 10.3390/ijms22010048.

93. Rossi C, Lanuti P, Cicalini I, De Bellis D, Pierdomenico L, Del Boccio P, Zucchelli M, Natale L, Sinjari B, Catitti G, Vespa S, Simeone P, Bologna G, Bucci I, Falasca K, Vecchiet J, Stuppia L, De Laurenzi V, Pieragostino D. BNT162b2 mRNA Vaccination Leads to Long-Term Protection from COVID-19 Disease. Vaccines (Basel). **2021** Oct 12;9(10):1164. doi: 10.3390/vaccines9101164
94. Brocco D, Simeone P, Marino PD, De Bellis D, D'Ascanio F, Colasante G, Grassadonia A, De Tursi M, Florio R, Di Ianni M, Cama A, Tinari N, Lanuti P. Low Phosphatidylserine+ Cells Within the CD34+/CD45dim/CD117(c-kit)+ Subpopulation Are Associated with Poor Outcomes in Metastatic Colorectal Cancer. Cancers (Basel). **2025** Feb 2;17(3):499. doi: 10.3390/cancers17030499.
95. Cossarizza A, Chang HD, Radbruch A, Acs A, Adam D, Adam-Klages S, Agace WW, Aghaeepour N, Akdis M, Allez M, Almeida LN, Alvisi G, Anderson G, Andrä I, Annunziato F, Anselmo A, Bacher P, Baldari CT, Bari S, Barnaba V, Barros-Martins J, et al. Guidelines for the use of flow cytometry and cell sorting in immunological studies (second edition). Eur J Immunol. **2019** Oct;49(10):1457-1973. doi: 10.1002/eji.201970107
96. Vespa S, Simeone P, Catitti G, Buca D, De Bellis D, Pierdomenico L, Pieragostino D, Cicalini I, Del Boccio P, Natale L, Owens T, Khorooshi R, De Laurenzi V, Stuppia L, Lanuti P. SARS-CoV-2 and Immunity: Natural Infection Compared with Vaccination. Int J Mol Sci. **2022** Aug 11;23(16):8982. doi: 10.3390/ijms23168982.
97. Vespa S, Del Biondo P, Simeone P, Cavallucci E, Catitti G, Auciello R, De Bellis D, Altomare I, Pierdomenico L, Canonico B, Cicalini I, Angilletta I, Del Boccio P, Pieragostino D, Santilli F, Urbani A, De Laurenzi V, Stuppia L, Lanuti P. Basophil Activation Test with Different Polyethylene Glycols in Patients with Suspected PEG Hypersensitivity Reactions. Int J Mol Sci. **2022** Nov 23;23(23):14592. doi: 10.3390/ijms232314592
98. Deer EL, González-Hernández J, Coursen JD, Shea JE, Ngatia J, Scaife CL, Firpo MA, Mulvihill SJ. Phenotype and genotype of pancreatic cancer cell lines. Pancreas. 2010

May;39(4):425-35. doi: 10.1097/MPA.0b013e3181c15963. Erratum in: Pancreas. **2018** Jul;47(6):e37. doi: 10.1097/MPA.0000000000001087

99. Masoud R, Reyes-Castellanos G, Lac S, Garcia J, Dou S, Shintu L, Abdel Hadi N, Gicquel T, El Kaoutari A, Diémé B, Tranchida F, Cormareche L, Borge L, Gayet O, Pasquier E, Dusetti N, Iovanna J, Carrier A. Targeting Mitochondrial Complex I Overcomes Chemoresistance in High OXPHOS Pancreatic Cancer. Cell Rep Med. **2020** Nov 17;1(8):100143. doi: 10.1016/j.xcrm.2020.100143.

100. Yoo I, Ahn I, Lee J, Lee N. Extracellular flux assay (Seahorse assay): Diverse applications in metabolic research across biological disciplines. Mol Cells. **2024** Aug;47(8):100095. doi: 10.1016/j.mocell.2024.100095.

101. Wang, S., Long, H., Hou, L. et al. The mitophagy pathway and its implications in human diseases. *Sig Transduct Target Ther.* **2023**; 8, 304. doi: 10.1038/s41392-023-01503-7

102. Ying H, Kimmelman AC, Lyssiotis CA, Hua S, Chu GC, Fletcher-Sananikone E, Locasale JW, Son J, Zhang H, Coloff JL, Yan H, Wang W, Chen S, Viale A, Zheng H, Paik JH, Lim C, Guimaraes AR, Martin ES, Chang J, Hezel AF, Perry SR, Hu J, Gan B, Xiao Y, Asara JM, Weissleder R, Wang YA, Chin L, Cantley LC, DePinho RA. Oncogenic Kras maintains pancreatic tumors through regulation of anabolic glucose metabolism. Cell. **2012** Apr 27;149(3):656-70. doi: 10.1016/j.cell.2012.01.058.

103. Hallin J, Bowcut V, Calinisan A, Briere DM, Hargis L, Engstrom LD, et al. Anti-tumor efficacy of a potent and selective non-covalent KRAS(G12D) inhibitor. Nature medicine **2022**;28(10):2171–82 doi 10.1038/s41591-022-02007-7

104. Ghiglione N, Abbo D, Bushunova A, Costamagna A, Porporato PE, Martini M. Metabolic plasticity in pancreatic cancer: The mitochondrial connection. Mol Metab. **2025** Feb;92:102089. doi: 10.1016/j.molmet.2024.102089.

105. Tape CJ, Ling S, Dimitriadi M, McMahon KM, Worboys JD, Leong HS, Norrie IC, Miller CJ, Poulogiannis G, Lauffenburger DA, Jørgensen C. Oncogenic KRAS Regulates Tumor Cell Signaling via Stromal Reciprocation. Cell. **2016** May 5;165(4):910-20. doi: 10.1016/j.cell.2016.03.029. Epub 2016 Apr 14. Erratum in: Cell. 2016 Jun 16;165(7):1818. doi: 10.1016/j.cell.2016.05.079.

106. Hanahan D., Weinberg R.A. Hallmarks of cancer: the next generation. Cell. **2011**;144:646–674. doi: 10.1016/j.cell.2011.02.013.

107. Zhou, G., Li, R., Sheng, S. *et al.* Organoids and organoid extracellular vesicles-based disease treatment strategies. *J Nanobiotechnol.* **2024**; 22, 679. doi: 10.1186/s12951-024-02917-3

108. Tay SP, Yeo CW, Chai C, Chua PJ, Tan HM, Ang AX, Yip DL, Sung JX, Tan PH, Bay BH, Wong SH, Tang C, Tan JM, Lim KL. Parkin enhances the expression of cyclin-dependent kinase 6 and negatively regulates the proliferation of breast cancer cells. J Biol Chem. **2010** Sep 17;285(38):29231-8. doi: 10.1074/jbc.M110.108241

109. Poulogiannis G, McIntyre RE, Dimitriadi M, Apps JR, Wilson CH, Ichimura K, Luo F, Cantley LC, Wyllie AH, Adams DJ, Arends MJ. PARK2 deletions occur frequently in sporadic colorectal cancer and accelerate adenoma development in Apc mutant mice. Proc Natl Acad Sci U S A. **2010** Aug 24;107(34):15145-50. doi: 10.1073/pnas.1009941107.

110. D'Amico AG, Maugeri G, Magro G, Salvatorelli L, Drago F, D'Agata V. Expression pattern of parkin isoforms in lung adenocarcinomas. Tumour Biol. **2015** Jul;36(7):5133-41. doi: 10.1007/s13277-015-3166-z.

111. Veeriah S, Taylor BS, Meng S, Fang F, Yilmaz E, Vivanco I, Janakiraman M, Schultz N, Hanrahan AJ, Pao W, Ladanyi M, Sander C, Heguy A, Holland EC, Paty PB, Mischel PS, Liau L, Cloughesy TF, Mellinghoff IK, Solit DB, Chan TA. Somatic mutations of the Parkinson's disease-associated gene PARK2 in glioblastoma and other human malignancies. Nat Genet. **2010** Jan;42(1):77-82. doi: 10.1038/ng.491.

112. Hu HH, Kannengiesser C, Lesage S, André J, Mourah S, Michel L, Descamps V, Basset-Seguin N, Bagot M, Bensussan A, Lebbé C, Deschamps L, Saiag P, Leccia MT, Bressac-de-Paillerets B, Tsalamlal A, Kumar R, Klebe S, Grandchamp B, Andrieu-Abadie N, Thomas L, Brice A, Dumaz N, Soufir N. PARKIN Inactivation Links Parkinson's Disease to Melanoma. J Natl Cancer Inst. **2015** Dec 17;108(3). doi: 10.1093/jnci/djv340.

113. Okami J, Simeone DM, Logsdon CD. Silencing of the hypoxia-inducible cell death protein BNIP3 in pancreatic cancer. Cancer Res. **2004** Aug 1;64(15):5338-46. doi: 10.1158/0008-5472.CAN-04-0089.

114. Tello D, Balsa E, Acosta-Iborra B, Fuertes-Yebra E, Elorza A, Ordóñez Á, Corral-Escariz M, Soro I, López-Bernardo E, Perales-Clemente E, Martínez-Ruiz A, Enríquez JA, Aragonés J, Cadenas S, Landázuri MO. Induction of the mitochondrial NDUFA4L2 protein by HIF-1α decreases oxygen consumption by inhibiting Complex I activity. Cell Metab. **2011** Dec 7;14(6):768-79. doi: 10.1016/j.cmet.2011.10.008.

115. Ikeda H, Kawase K, Nishi T, Watanabe T, Takenaga K, Inozume T, Ishino T, Aki S, Lin J, Kawashima S, Nagasaki J, Ueda Y, Suzuki S, Makinoshima H, Itami M, Nakamura Y, Tatsumi Y, Suenaga Y, Morinaga T, Honobe-Tabuchi A, Ohnuma T, Kawamura T, Umeda Y, Nakamura Y, Kiniwa Y, Ichihara E, Hayashi H, Ikeda JI, Hanazawa T, Toyooka S, Mano H, Suzuki T, Osawa T, Kawazu M, Togashi Y. Immune evasion through mitochondrial transfer in the tumour microenvironment. Nature. **2025** Feb;638(8049):225-236. doi: 10.1038/s41586-024-08439-0. Epub 2025 Jan 22. Erratum in: Nature. 2025 Aug;644(8076):E33. doi: 10.1038/s41586-025-09408-x.

116. Gagliardi S, Mitruccio M, Di Corato R, Romano R, Aloisi A, Rinaldi R, Alifano P, Guerra F, Bucci C. Defects of mitochondria-lysosomes communication induce secretion of mitochondria-derived vesicles and drive chemoresistance in ovarian cancer cells. Cell Commun Signal. **2024** Mar 6;22(1):165. doi: 10.1186/s12964-024-01507-y.

117. Mullard A. Cancer cells 'poison' the immune system with tainted mitochondria. **2025** Jan 22 doi: 10.1038/d41586-025-00176-2

118. Vikramdeo KS, Anand S, Khan MA, Khushman M, Heslin MJ, Singh S, Singh AP, Dasgupta S. Detection of mitochondrial DNA mutations in circulating mitochondria-originated extracellular vesicles for potential diagnostic applications in pancreatic adenocarcinoma. Sci Rep. 2022 Nov 2;12(1):18455. doi: 10.1038/s41598-022-22006-5.

119. NCT05737706

120. Wei D, Wang L, Zuo X, Maitra A, Bresalier RS. A Small Molecule with Big Impact: MRTX1133 Targets the KRASG12D Mutation in Pancreatic Cancer. Clin Cancer Res. **2024** Feb 16;30(4):655-662. doi: 10.1158/1078-0432.CCR-23-2098.

121. Han L, Meng L, Liu J, Xie Y, Kang R, Klionsky DJ, Tang D, Jia Y, Dai E. Macroautophagy/autophagy promotes resistance to $KRAS^{G12D}$-targeted therapy through

glutathione synthesis. Cancer Lett. **2024** Nov 1;604:217258. doi: 10.1016/j.canlet.2024.217258.

122. Sliter DA, Martinez J, Hao L, Chen X, Sun N, Fischer TD, Burman JL, Li Y, Zhang Z, Narendra DP, Cai H, Borsche M, Klein C, Youle RJ. Retraction Note: Parkin and PINK1 mitigate STING-induced inflammation. Nature. **2025** Aug;644(8078):1116. doi: 10.1038/s41586-025-09346-8.

123. Rabas N, Palmer S, Mitchell L, Ismail S, Gohlke A, Riley JS, Tait SWG, Gammage P, Soares LL, Macpherson IR, Norman JC. PINK1 drives production of mtDNA-containing extracellular vesicles to promote invasiveness. J Cell Biol. **2021** Dec 6;220(12):e202006049. doi: 10.1083/jcb.202006049.

124. Wong FC, Merker SR, Bauer L, Han Y, Le VMH, Wenzel C, Böthig L, Heiduk M, Drobisch P, Rao VS, Malekian F, Mansourkiaei A, Sperling C, Polster H, Pecqueux M, Istvanffy R, Ye L, Kong B, Aust DE, Baretton G, Seifert L, Seifert AM, Weitz J, Demir IE, Kahlert C. Extracellular vesicles from pancreatic cancer and its tumour microenvironment promote increased Schwann cell migration. Br J Cancer. **2025** Mar;132(4):326-339. doi: 10.1038/s41416-024-02915-0.